Report
R-15-05
September 2015

Microbial sulphide-producing activity in MX-80 bentonite at 1750 and 2000 kg m^{-3} wet density

Andreas Bengtsson
Johanna Edlund
Björn Hallbeck
Carl Heed
Karsten Pedersen

SVENSK KÄRNBRÄNSLEHANTERING AB

SWEDISH NUCLEAR FUEL
AND WASTE MANAGEMENT CO

Box 250, SE-101 24 Stockholm
Phone +46 8 459 84 00
skb.se

SVENSK KÄRNBRÄNSLEHANTERING

ISSN 1402-3091
SKB R-15-05
ID 1469121

September 2015

Microbial sulphide-producing activity in MX-80 bentonite at 1750 and 2000 kg m^{-3} wet density

Andreas Bengtsson, Johanna Edlund, Björn Hallbeck,
Carl Heed, Karsten Pedersen
Microbial Analytics Sweden AB

Abstract

In the Swedish model for geodisposal of spent nuclear fuel the bentonite barrier has an important function in maintaining the integrity of the copper canisters isolating the spent fuel. The bentonite is intended to hinder outward transport of radionuclides and inward transport of corrosive groundwater components, and also act as a buffer against rock movements. Sulphate-reducing bacteria (SRB) in the surrounding groundwater and naturally residing in the bentonite could harm the canister by production of corrosive sulphide (S^{2-}) by reduction of sulphate (SO_4^{2-}). A strong limiting factor for microbial activity is the density related swelling pressure of the buffer. In the repository a highly compacted bentonite with a bulk wet density between 1,950 and 2,050 kg m^{-3} and a corresponding swelling pressure of ~5 MPa at full water saturation is planned to be used. In this experiment we investigated how microbial sulphide-producing activity was influenced by a low (1,750 kg m^{-3}) and a high (2,000 kg m^{-3}) buffer wet density when all other variables were kept favourable for growth and activity of SRB.

Ten identical test cells were used in the experiment which consisted of a titanium cylinder with a piston inside. The cells were filled with Wyoming MX-80 bentonite clay powder with addition of a bacterial cocktail consisting of three different species of SRB (except sterile controls). By tightening screws running through a lid on top of the piston and thereby forcing the piston downwards the amount of pressure acting on the clay could be regulated and also monitored by a force transducer connected to a data collection system. Five of the test cells were adjusted to a wet density of 1,750 kg m^{-3} and 0.7 MPa and the other five test cells were adjusted to 2,000 kg m^{-3} and 5 MPa during simultaneous water saturation with a salt solution without carbon source through an inlet at the bottom of the test cells. After approximately 70 days when the clay had reached the planned wet densities and was fully water saturated, the piston and bottom lid were removed. A 40 µm pore size titanium filter was attached to the bottom lid and kept the clay from swelling out into the inlet hole. This filter was replaced with a copper disc that simulated a copper canister at start of the experiments. On the opposite clay core side to the copper disc, $^{35}SO_4^{2-}$ together with lactate was added. The test cells were then closed again and the force transducer, piston and top lid were refitted. The test cells were sampled after 47, 77 and 123 days from the addition of $^{35}SO_4^{2-}$, SO_4^{2-} and lactate. The radioactivity of the $Cu_x{}^{35}S$ that had formed on the copper discs was localized and quantified using electronic autoradiography. Samples were taken from different layers of the clay core and analysed for distribution of ^{35}S, most probable number of SRB and distribution of SO_4^{2-}.

Approximately 10,000 times higher surface radioactivity was measured on the 1,750 kg m^{-3} discs compared to the 2,000 kg m^{-3} discs. The calculated rate of SO_4^{2-} to S^{2-} reduction was also much higher in the 1,750 kg m^{-3} cells. Heat treatment of the clay did not have any significant sterilization effect in the 1,750 kg m^{-3} cells where cells with addition of microbes showed similar levels of radioactivity on the discs compared to the discs in 1,750 kg m^{-3} cells with heat treated clay. In the 2,000 kg m^{-3} case the cells with added microbes showed a low level of sulphide-producing activity and the heat treated cells did not show any measurable radioactivity on their discs. Results from MPN analysis matched results from radioactivity measurements on the copper discs to some extent. In the 1,750 cases (added microbes or not) an increasing trend was found, with relatively high bacterial numbers from the latest sampling at 123 days compared to day 47. For the 2,000 kg m^{-3} case, low numbers or values below detection of cultivable SRB were found in the test cells. An uneven SO_4^{2-} distribution through the clay was observed with lower values closest to the copper disc, probably due to a wash out effect during water saturation. This effect was more pronounced in the 2,000 kg m^{-3} test cells. To avoid this effect in future experiments the water saturation medium could be added from both sides of the clay core. The added $^{35}SO_4^{2-}$ on the other hand diffused readily through the all test cells. This experiment showed that bacteria truly are opportunistic life forms that can take advantage of the seemingly small density decrease from 2,000 to 1,750 kg m^{-3} and that they are able to proliferate in an otherwise harsh environment.

Contents

Abbreviations used in the report

Abbreviation	Meaning
SRB	Sulphate-reducing bacteria
DSMZ	German collection of microorganisms and cell cultures
AODC	Acridine orange direct count method
PEEK	Polyether-ether-ether-ketone (organic thermoplastic polymer)
gdw	Gram dry weight
gww	Gram wet weight
AGW	Analytical grade water
MPN	Most probable number
LSC	Liquid scintillation counting
RedRate	Rate of SO_4^{2-} to S^{2-} reduction
cpm	Counts per minute
dps	Disintegrations per second

1 Introduction

Microbial activity has been demonstrated to decrease with increasing density and swelling pressure of bentonite clays (Motamedi et al. 1996, Stroes-Gascoyne et al. 1997, Motamedi 1999). Previous work with Wyoming MX-80 bentonite suggests that microbial sulphide-producing activity and cultivability cease somewhere in the range of 1,900–2,100 kg m^{-3} wet density but the exact cut-off density remains to determine (Pedersen et al. 2000a, b, Masurat et al. 2010b). Variables of importance for such activity, in addition to clay density and swelling pressure can be pore space and pore water composition, transport conditions to and from the buffer boundaries, usability of the naturally occurring organic matter present in the clay and H_2 from corroding metals, and temperature.

The goal with this work was:

- Identification of a possible threshold buffer wet density with a corresponding swelling pressure above which microbial sulphide-producing activity is practically inhibited (all others conditions being favourable for the microbes) and evaluation of how microbial sulphide-producing activity decreases as wet density and swelling pressure increase.

1.1 Microbial S^{2-} production rate – a scoping calculation

A sulphate-reducing bacterium can produce up to $1–2 \cdot 10^{-15}$ mole S^{2-} from SO_4^{2-} per hour (Jørgensen 1978, Hallbeck 2014). It has been shown that sulphate-reducing bacteria (SRB) in deep groundwater can keep up with this rate when provided with H_2 at concentrations not much higher than 1 μM (Pedersen 2012a, b). Analysis of numbers of SRB in commercial MX-80 bentonite showed 0.13 cultivable SRB mg^{-1} clay during the alternative buffer material project at Äspö (Svensson et al. 2011). With 350 mm of bentonite surrounding the canister at a density of 2,000 kg m^{-3}, there will be approximately 50 SRB mm^{-2} of canister surface that have the potential to produce $10^2 \cdot 10^{-15}$ mole S^{2-} mm^{-2} h^{-1} which could cause problems for the sustainability of a high-level radioactive waste disposal canister in a long time span of 100,000 years or more. Although this number is conservative and comes with very large uncertainty, this number demonstrates that it does not take very many SRB per volume of buffer to challenge the integrity of the canister. If given good growth conditions, i.e. carbon and energy sources and SO_4^{2-}, the SRB can rapidly multiply several orders of magnitude and then the produced S^{2-} over time may become far too large. Therefore, it is required to confirm the present hypothesis that sulphide producing activity of SRB will be very slow or nil in the planned buffer wet density range and concomitant swelling pressures.

1.2 Method for detection of microbial sulphide-production in buffer

Based on previous results (Pedersen 2010), it is expected that there will be very low microbial sulphate producing activity when the clay wet density approaches the planned 2,000 kg m^{-3}, which put a very low detection limit demand on the applied methods. For this purpose, the use of radiotracers is one of the best methodological alternatives. Among those, the use of $^{35}SO_4^{2-}$ for detection of microbial sulphide-production to $^{35}S^{2-}$ from $^{35}SO_4^{2-}$ is the most sensitive method available due to the short half-life of this sulphur isotope (87.4 days). This method has been used in clay environments with good results previously (Pedersen et al. 2000b, Pedersen 2010).

Earlier, some experiments were designed with free water in contact with the clay core (Pedersen 2010). This layout allowed bacterial sulphide-producing activity to proceed outside the clay core which may, or may not, have masked a slow bacterial sulphide-producing activity in the compacted clay core. It was concluded that future experiments must exclude free water in contact with the clay core to better mimic the repository situation; a requirement that was achieved in this experiment by an upgrade of the test cell design and experimental procedures. The experimental design in this work consisted of test cells made of titanium in which MX-80 bentonite clay cores were installed

together with SRB, copper discs and additions needed for SRB sulphide producing activity, and then incubated under relevant conditions. In this work we investigated how microbial sulphide-producing activity was influenced by a low (1,750 kg m^{-3}) and a high (2,000 kg m^{-3}) Wyoming MX-80 bentonite buffer wet density with corresponding swelling pressures of 0.7 and 5 MPa, respectively, when all other variables were kept favourable for growth and sulphide-producing activity of SRB.

2 Material and method

2.1 Test cells

Ten identical test cells were used in the experiment. A test cell consisted of a titanium cylinder with top and bottom lid attached by six Allen screws for each lid. A piston equipped with a removable ventilation plug operated inside the cylinder (Figure 2-1). When the piston is at its most extended position, a 35×20 mm cavity is produced inside of the cylinder (Figure 2-2). This cavity was filled with Wyoming MX-80 bentonite clay powder (see section 2.4). By tightening the screws running through the top lid and thereby forcing the piston downwards the amount of pressure acting on the clay could be regulated. To register the exact pressure acting on the clay, a force transducer connected to a data collection system was mounted between the top lid and the top of the piston (see section 2.2). During the water saturation phase of the experiment (described in detail in section 2.5) a saturation bottom lid was used. The lid had a 2 mm inlet hole which allowed fluid to enter the test cell and reach the clay. To stop the clay from swelling out through the inlet hole, and also to get an evenly distributed inlet flow, a 40 µm pore size titanium filter was mounted with two Phillips screws on the inside of the saturation lid. After the saturation phase the bottom lid was replaced with a lid without inlet and the titanium filter was replaced with a copper disc (see section 2.6 for details).

2.2 Force transducer and data collection

The force transducers used to register the swelling pressure from the bentonite clay were purchased from Stig Wahlström Automatik, Stockholm, Sweden. Ten force transducers were used, one for each test cell. Five force transducers had a load range from 0 to 500 lbs (AL131CR, Honeywell model 53) and 5 force transducers has a load range from 0 to 2,000 lbs (AL131DL, Honeywell model 53). The force transducers were connected to a data collection system consisting of ten transducer amplifiers for strain gage (Stig Wahlström Automatik, model DR7DC), a programmable logic controller (model Direct Logic 06) and a PC with a custom built software (CRS Reactor Engineering, Stenkullen, Sweden) for calibration and monitoring of the force transducer signals.

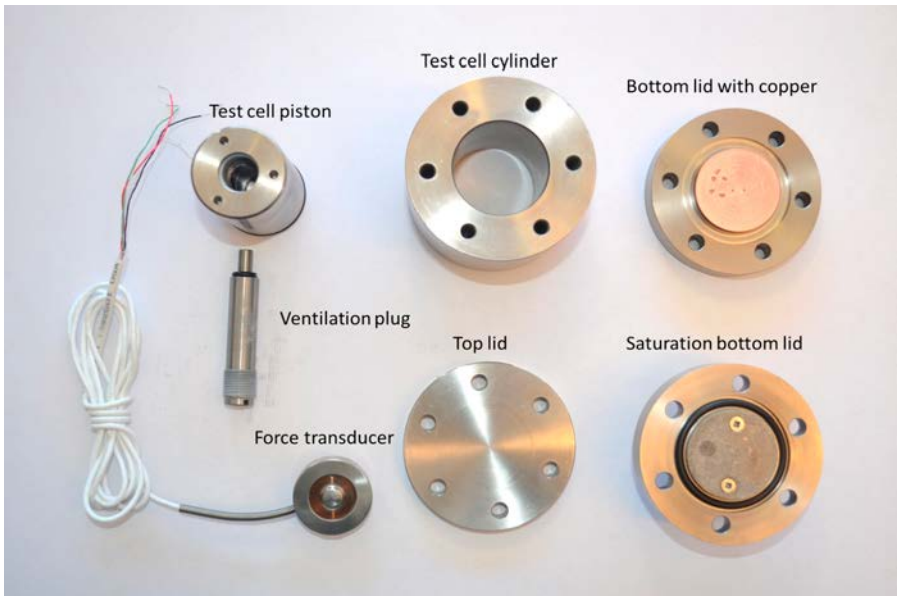

Figure 2-1. *Exploded view of a test cell.*

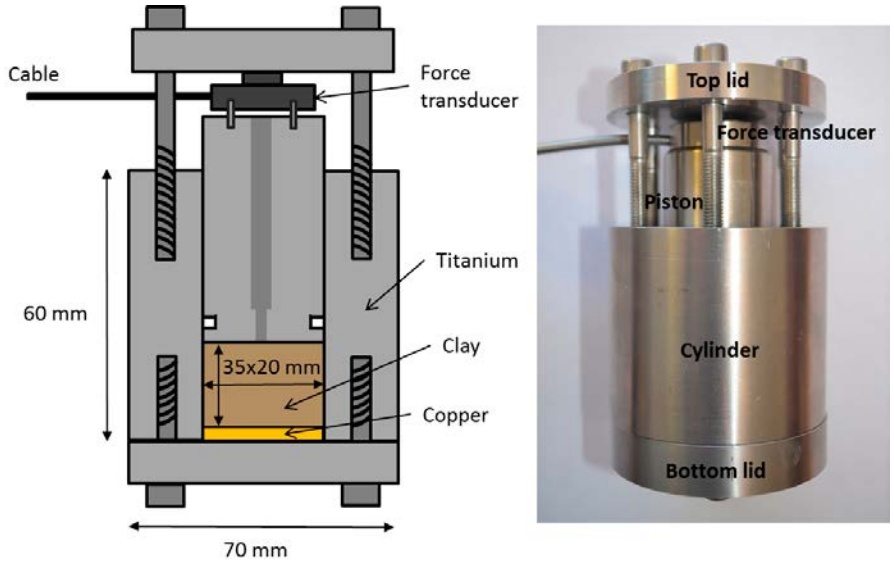

Figure 2-2. *Left: A schematic cross section of a test cell. Right: An assembled test cell.*

2.3 Bentonite clay slurries

Three different species of SRB were used in the experiment. *Desulfovibrio aespoeensis* (DSM 10631), *Desulfotomaculum nigrificans* (DSM 574) and *Desulfosporosinus orientis* (DSM 765). *D. aespoeensis* was isolated from deep groundwater (Motamedi and Pedersen 1998), *D. nigrificans* is a thermophilic, spore-forming sulphide-producing bacterium and *D. orientis* is spore-forming with the ability to grow with H_2 as source of energy. The bacteria were grown in appropriate media and temperature as specified by the German collection of microorganisms and cell cultures (DSMZ). At the start day of the experiments bacterial numbers for each of the three bacterial cultures were determined in 1 mL samples using the acridine orange direct count (AODC) method as devised by Hobbie et al. (1977) and modified by Pedersen and Ekendahl (1990).

Sixty grams of bentonite clay powder was dispersed in 1,110 mL sterile anaerobic water inside an anaerobic box with an atmosphere consisting of 97% N_2 and 3% H_2 (COY Laboratory Products, Grass Lake, MI, USA). Thirty mL of each of the three bacterial cultures were added and mixed with the dispersed bentonite clay. The bentonite clay slurry was then dried in large glass petri dishes inside the anaerobic box until the clay adopted a gel texture. The petri dishes were then taken out of the anaerobic box and placed in a fume hood to let the clay dry completely. The dried clay was scraped up using sterile spoons and then carefully grinded in a mortar to a fine powder. The grinded clay was mixed with 540 g of bentonite clay powder, creating a batch of 600 g of bentonite clay powder with $5 \cdot 10^6$ SRB gdw^{-1} (SRB per gram dry weight). Another 300 g of bentonite clay powder was heat treated in a laboratory heating oven at 110°C for a week with the purpose to sterilize the clay. This batch was used in four test cells as negative controls (Table 2-1).

2.4 Compaction of bentonite clay

The day before compaction of the clay the water content was determined in both the sterile and the SRB-doped bentonite clay batches by heating 3×1 g of each batch in aluminium bowls in 105°C overnight. An average of the weight difference before and after heating was thus taken the water content for each clay batch.

The clays were thereafter transported to Clay Technology AB in Lund, Sweden in air tight plastic containers so that they would remain dry without water until compaction. The compaction was performed by Clay Technology personnel to produce two different clay wet densities; five test cells with 1,750 kg m^{-3} and another five test cells with 2,000 kg m^{-3}. Two test cells of each density were loaded with heat treated bentonite clay and the remaining six test cells contained clay with added microbes (Table 2-1).

Table 2-1. Set of test cells with clay density and clay treatment.

Test cell number	Intended clay density (kg m^{-3})	Treatment	Additions (similar for all test cells) (pore water conc.)
1 and 2	1,750	Heat treated	0.06 µM $^{35}SO_4^{2-}$ 0.13 mM SO_4^{2-} 28 mM NaC_3H_5O
3, 4 and 5	1,750	Added microbes	
6 and 7	2,000	Heat treated	
8, 9 and 10	2,000	Added microbes	

2.5 Water saturation of bentonite clay

After compaction of the bentonite clay the test cells were assembled with the top plates, force transducers and the water saturation bottom lid and then mounted on a custom built water saturation system (Figure 2-3). To verify that the system was gas tight, helium was flushed into the system and every coupling was sniffed with a helium leak detector. The system was then alternately evacuated to < 10 Pa total pressure and filled with nitrogen to remove all O_2. When the system was free from O_2 it was left in an evacuated state and a sterile, modified anaerobic SRB growth medium was pushed into the system with 200 kPa total pressure. The medium was prepared without lactate, SO_4^{2-} and S^{2-} as described in Table 2-2. It was mixed as described by Widdel and Bak (1992) for preparing anoxic media and modified as described elsewhere (Hallbeck and Pedersen 2008). The medium was delivered to the test cells by a pressure transmitting device consisting of a steel cylinder with piston made of poly-ether-ether-ketone (PEEK) that was pressurized by N_2 gas on one side of the piston. The other side of the piston was filled with the medium under anaerobic conditions. Every tube and pressure transmitter used for the water saturation with the medium was sterilized in an autoclave at 121°C for 20 minutes before use.

Table 2-2. Water saturation medium recipe.

Addition	Amount
Analytical grade water (mL)	1,000
NaCl (g L^{-1})	7.0
$CaCl_2 \cdot 2H_2O$ (g L^{-1})	1.0
KCl (g L^{-1})	0.67
NH_4Cl (g L^{-1})	1.0
KH_2PO_4 (g L^{-1})	0.15
$MgCl_2 \cdot 6H_2O$ (g L^{-1})	0.5

Figure 2-3. *Water saturation system with ten mounted test cells positioned upside down.*

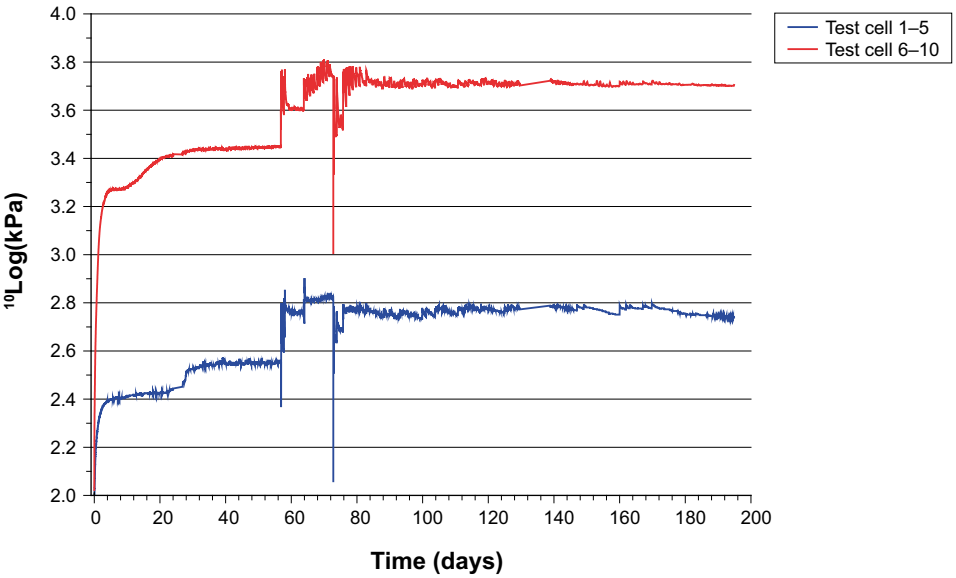

Figure 2-4. *Average pressure of test cell 1–5 (1,750 kg m^{-3}) and test cell 6-10 (2,000 kg m^{-3}). The pressure drop at 72 days occurred when the test cells were opened for addition of copper discs, $^{35}SO_4^{2-}$ and carbon source. For absolute values see Appendix A.1.*

The pressures created by the swelling clays were monitored and the screws running through the top lids were adjusted on daily basis for 10 weeks so that correct swelling pressures for the two different clay densities at full water saturation were obtained. An average of the swelling pressures from the two densities is shown in Figure 2-4. Water was allowed to move freely in and out of the clay during the saturation phase.

Given the time the samples were allowed to water saturate and by considering the swelling pressures registered by the force transducers, the degree of water saturation was deemed to be 100%. The water contents listed in Table 2-3 were used for calculations and interpretations of results for 1,750 kg m^{-3} and the 2,000 kg m^{-3} clay samples, respectively.

2.6 Addition of $^{35}SO_4^{2-}$ and carbon source

All work performed with additions of $^{35}SO_4^{2-}$ and carbon source as well as the cleaning and insertion of the copper discs were carried out in the anaerobic box.

Ten copper discs were cleaned in an ultrasonic bath for 5 min in 99% ethanol and then rinsed with sterile analytical grade water (AGW) (Millipore Elix Essential 3, Millipore, Solna, Sweden). Afterwards the discs were placed in a beaker containing 250 mL gently stirred 0.5 M sulfamic acid (aminosulfonic acid, H_2NSO_3H) (cat.nr. 24 277-2, Sigma-Aldrich) for 24 h, according to procedures for chemical cleaning of copper in ISO 8407:2010 – Corrosion of metals and alloys – Removal of corrosion products from corrosion test specimens (ISO 847:2009, IDT). The procedure was finished by sequentially washing the discs four times in glass beakers containing 400 mL sterilized, anoxic AGW at pH 7.

The test cells were disconnected from the water saturation system and the bottom lids with titanium filters, together with top lids and force transducers were removed. In each cell a same sized copper disc was inserted in the cavity that the titanium filter left in the clay. A new bottom lid without inlet was attached to each cell. The ventilation plugs in the middle of the pistons were thereafter unscrewed to be able to remove the pistons. The radioactive sulphur isotope $^{35}SO_4^{2-}$ (PerkinElmer, cat. no. NEX041H010MC, 10mCi (370 MBq), specific activity: 1050–1600Ci (38.8–59.2 TBq)/mmol, sodium sulphate in 1 mL water) was then added by pipette to a final concentration of 0.06 µM in the pore water contained in each test cell to four equally spaced points on the clay core surface. In addition, a SO_4^{2-} solution was added to give a pore water concentration of 0.13 mM together with a 5.7 M lactate solution to a final a pore water concentration of 28 mM in all test cells. The test cells were then reassembled

with piston, force transducers and top lids. By simultaneously observing the data produced by the force transducers and adjusting the screws running through the top lid, the same swelling pressure as before opening of the cells was set (Figure 2-4).

2.7 Sampling and analysis

After 47, 77 and 123 days from the addition of $SO_4^{2-}$and lactate test cell 3 and 8, test cell 4 and 9 and test cell 1, 2, 5, 6, 7 and 10 were sampled, respectively. Each test cell was given a code with information of the clay wet density, addition of microbes and incubation time: T = test cell, 1,750/2,000 = 1,750 or 2,000 kg m^{-3} clay wet density, (+/−) = with or without adding of microbes, d = days of incubation. E.g. for test cell 1 the code will be: T1 1750 (−) 123d (Table 2-3).

The logging in the force transducer software were stopped, the force transducer was removed together with the top lid and screws. The top lid was then attached again, however with shorter screws to be able to push the piston all the way to the bottom. The test cells were moved to a fume hood and the bottom plates were carefully removed. The piston was then carefully pressed up by turning the screws so that the edge of the copper disc became visible (Figure 2-5). An overview of analyses carried out on the copper discs and the clay cores is shown in Table 2-4.

Table 2-3. Weight and volume parameters set at start of the experiments for the MX-80 bentonite clay in each test cell.

Test cell code	Test cell volume (cm^3)	Amount of clay (gdw)	Pore water volume (mL)	Water content (% gww)
T1 1750 (−) 123d	19.23	22.7	11.06	32.77
T2 1750 (−) 123d	19.23	22.7	11.06	32.77
T3 1750 (+) 47d	19.23	23.2	10.88	31.93
T4 1750 (+) 77d	19.23	23.2	10.88	31.93
T5 1750 (+) 123d	19.23	23.2	10.88	31.93
T6 2000 (−) 123d	19.23	30.24	8.35	21.64
T7 2000 (−) 123d	19.23	30.24	8.35	21.64
T8 2000 (+) 47d	19.23	30.93	8.10	20.76
T9 2000 (+) 77d	19.23	30.93	8.10	20.76
T10 2000 (+) 123d	19.23	30.93	8.10	20.76

Figure 2-5. *Sampling of test cell 8 (T8 2000 (+) 47d). Left: pushing the piston up by tightening screws. Right: copper disc completely pushed out of the test cell.*

Table 2-4. Overview of performed analyses.

Analysis	Method
$Cu_x{}^{35}S$ on copper discs	Surface autoradiography
Most probable number	Cultivation
Distribution of ^{35}S in clay cores	Liquid scintillation counting
Distribution of SO_4^{2-} in clay cores	Turbidimetric method by precipitation of $BaSO_4$

2.7.1 Copper discs

The copper discs were removed with sterile tweezers and put in sterile Petri dishes and then immediately transferred to the anaerobic box where the Petri dishes were filled with anaerobic sterile AGW to completely cover the discs in order to remove clay residues and $^{35}SO_4^{2-}$. The discs were left in the Petri dishes overnight.

Next day the discs were rinsed with sterile anaerobic AGW 5 times in separate beakers and then left to air dry outside of the anaerobic box. When dried, the radioactivity of the $Cu_x{}^{35}S$ that had formed on the copper plates was localized and quantified using a Packard Instant Imager electronic autoradiography system (Packard Instrument Company, Meriden, CT, USA) as follows. The copper plates were first placed on a foam sheet that was used to obtain a uniform plate level in the imager. The Instant Imager was calibrated according to the manufacturer's instructions using a ^{14}C calibration source provided by the manufacturer (Packard). The scanning time in the Instant Imager was set to 30 min. The Instant Imager sampled radioactivity in 0.5×0.5 mm pixels. Each pixel delivered a gross radioactivity count that was used for modelling and calculating the total amount of Cu_xS formed on the discs.

2.7.2 Bentonite clay samples

Bentonite clay samples were taken out in three positions for test cell 3 and 8; close to the copper disc, in the middle of the clay core and close to the piston. The positions were denoted 1, 2 and 3 where number 1 was close to the copper surface and so on. Samples at each position were taken for analysis of most probable number (MPN) of SRB, water content and distribution of ^{35}S and SO_4^{2-} in the clay (Figure 2-6).

For test cell 1, 2, 4, 5, 6, 7, 9 and 10 the clay sampling method was modified in the following manner. Distribution of ^{35}S and SO_4^{2-} were analysed from six different layers in the clay in contrast to 3 points as for test cell 3 and 8. The layers where: the first millimetre of clay closest to the copper surface (0–1 mm), the next four millimetres (1–5 mm), the next five millimetres (5–10 mm), the next five millimetres (10–15 mm), the next two and a half millimetres (15–17.5 mm) and the last two and a half millimetres (17.5–20 mm). This was done to get a more resolved data profile than that obtained for the sampled test cell 3 and 8. One gram samples for MPN-analysis were taken on millimetre 1, 5 and 10 in the centre of the clay core (Figure 2-6).

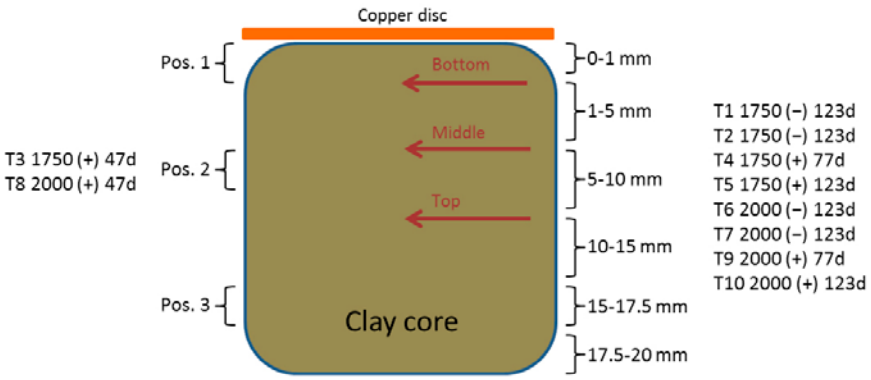

Figure 2-6. *Sampling positions and layers in clay cores. Left side describes sampling for test cell 3 and 8. Right side describes sampling for test cell 1, 2, 4, 5, 6, 7, 9 and 10. Red arrows indicate sampling positions for MPN and water content samples which only refers to test cell 1, 2, 4, 5, 6, 7, 9 and 10.*

2.7.2.1. MPN samples

Samples for MPN-analysis were transferred to the anaerobic box where tubes containing 1 gram wet weight (gww) samples were filled with 40 mL sterile anaerobic 0.9% NaCl solution and then put on shaker to disperse the bentonite clay. After the bentonite clay had dispersed (~2 h) the samples were inoculated in five tubes for each of total two 10-time dilutions, resulting in an approximate 95% confidence interval lower limit of 1/3 of the obtained value and an upper limit of three times the value (Greenberg et al. 1992). The cultivation tubes were filled with 9 mL anaerobic SRB growth medium, mixed as described by Widdel and Bak (1992) for preparing anoxic media and modified as described elsewhere (Hallbeck and Pedersen 2008). The MPN samples were cultured in 28°C for four weeks before analysis. SRB were detected by measuring S^{2-} production using the $CuSO_4$ method according to Widdel and Bak (1992) on a UV visible spectrophotometer (Genesys UV 10, Thermo Electron Corporation).

2.7.2.2. Distribution of ^{35}S in the clay core

Tubes containing bentonite clay samples for liquid scintillation counting (LSC) were kept in the fume hood after sampling and 40 mL of a sterile 10% $CaCl_2$ solution was added. The tubes were left for about a week to let the bentonite clay settle as a dispersed pellet in the bottom of the tubes. Afterwards, 100 µL of the supernatants were transferred to 24-mL scintillation vials (WHEA986581, VWR; Wheaton Industries, Stockholm, Sweden) containing 9.9 mL of a high-ionic scintillation cocktail (Biodegradable Counting Scintillant NBSC 104; Amersham Scientific). Counts per minute (cpm) for ^{35}S were measured in a Triathler LSC (Hidex, Turku, Finland), the counting time was 1 min. The scintillator's measuring efficiency was determined by analysing a 100 µL of $^{35}SO_4^{2-}$ (PerkinElmer, cat. no. NEX041H001MC, 1 mCi (37MBq), specific activity: 1050–1600Ci (38.8–59.2 TBq)/mmol, sodium sulphate in 1 mL water). The efficiency was 36%.

2.7.2.3. Distribution of SO_4^{2-} in the clay core

From the same tubes as in 2.7.2.2 SO_4^{2-}concentrations of the different positions or layers of the clay core were determined using the turbidimetric SulfaVer4 $BaSO_4$ precipitation method (Method #8051, HACH Lange, Sköndal, Sweden), after 10 times dilutions in AGW in order to obtain optimal concentration range for analyses. Analyses were measured on a HACH spectrophotometer model DR/2500 Odyssey (HACH Lange, Sköndal, Sweden). SO_4^{2-} analysis was also performed on raw bentonite clay before the start of the experiment to determine the naturally occurring SO_4^{2-} background value. This was done by dispersing 1 g of bentonite clay in 10, 20, 30, 40 and 50 mL of a 10% $MgCl_2$ solution. SO_4^{2-} was then measured with the SulfaVer4 method on diluted or undiluted supernatant from the five different tubes. To ensure that the entire SO_4^{2-} was leached from the bentonite clay the remaining supernatant after analysis was poured off and the experiment was repeated with new $MgCl_2$ solution. No SO_4^{2-} could be detected in any of the tubes after the first leach.

2.8 Determining the rate of SO_4^{2-} to S^{2-} reduction

First, consider a situation where the rate of SO_4^{2-} to S^{2-} reduction (RedRate) is known. Consider also that the following is known or assumed:

- The geometry of the clay core. This was known at the start of the experiment.
- The original amount of $^{35}SO_4^{2-}$ added and where it was applied. This was known at the start of the experiment.
- The diffusion coefficients for diffusion of SO_4^{2-} and S^{2-} through bentonite clay. The coefficient for SO_4^{2-} was assumed to be $2 \cdot 10^{-12}$ for bentonite clay compacted to 2,000 kg m^{-3} and $1.2 \cdot 10^{-11}$ for bentonite clay compacted to 1,750 kg m^{-3}. The coefficient for S^{2-} was assumed to be $4 \cdot 10^{-12}$ for bentonite clay compacted to 2,000 kg m^{-3} and $2.4 \cdot 10^{-11}$ for bentonite clay compacted to 1,750 kg m^{-3}. These values where modified in some instances to determine how those changes affected the end result for the value on SO_4^{2-} to S^{2-} reduction rate. See 2.8.3 for a description of this sensitivity analysis and 4.4 for discussion on selection of coefficients.
- The rate of decay of ^{35}S. This was known at the start of the experiment.
- SRB was evenly spread throughout the clay core during the experiment.

In this situation it is possible to determine the amount of $^{35}S^{2-}$ that reaches the copper plate at any given time by means of computer simulation of the changing conditions in the test cells. A mathematical model and a computer program was developed to perform such simulations. By running this program with different values on RedRate and comparing the resulting amounts of $^{35}S^{2-}$ on the copper plate in the mathematical model with the actual amounts found in the experiment test cells it was possible to determine values for RedRate for each test cell.

2.8.1 Mathematical model of test cells

The interior of the test cells were divided into a matrix of 51 cells in each direction. This means that 51×51×51 = 132,651 matrix cells were used to model a test cell where some matrix cells represented the test cell walls and the copper plate. (For the sensitivity analysis 31×31×31 = 29,791 cells were used.) The majority of the matrix cells represented bentonite clay. Each cell held an amount of $^{35}SO_4^{2-}$ and an amount of $^{35}S^{2-}$. Each matrix cell also contained SRB that converted SO_4^{2-} to S^{2-} at a rate of RedRate per volume and time. SO_4^{2-} and S^{2-} were not allowed to diffuse through the test cell walls in the model and the initial amounts of $^{35}SO_4^{2-}$ and $^{35}S^{2-}$ were set to 0 in all matrix cells except four. These four matrix cells were positioned on the top surface of the clay core in positions marked with red in Figure 2-7 and a total of 0.63 nmole and 0.49 nmole $^{35}SO_4^{2-}$ were added to the 1,750 and 2,000 kg m^{-3} test cells, respectively.

2.8.2 Simulation program

The computer program was based on the concept of dividing the test cell space into small parts (matrix cells) and repeatedly computing the changes in SO_4^{2-} and S^{2-} concentrations in each matrix cell during short time intervals (dT). This approach is called a finite difference method (Morton and Mayers 2005) and is known to be convergent and stable if the criterion: $dT < 0.5 \times (\text{cell thickness})^2/D_s$ is satisfied (Morton and Mayers 2005). In this convergence criterion D_s denotes the higher of the diffusion coefficients of SO_4^{2-} and S^{2-}. The computer program was written in the programming language Visual Basic 6 running under Windows Vista on a regular PC. The change in SO_4^{2-} concentration in each matrix cell during a time step (dT) was computed by adding the diffusion in/out of its adjacent matrix cells and subtracting the amount of SO_4^{2-} converted to S^{2-} during the dT. The change in S^{2-} concentrations was computed by adding the diffusion in/out of its adjacent matrix cells and adding the amount of S^{2-} converted from SO_4^{2-} during the dT. The diffusion between matrix cells during a dT was computed with Fick's law (Coulson and Richardson 1990, 446–447). One way of writing Fick's law is equation (2.1) below. The amount of SO_4^{2-} converted to S^{2-} during a dT (dSO4Red) was computed with equation (2.2) below.

$$m' = \Delta C * D * A/d \qquad \text{(Fick's law)} \qquad (2.1)$$

m' = mass transport (mol s^{-1})

ΔC = concentration difference between cells (mol m^{-3})

D = diffusion coefficient (m^2 s^{-1})

A = surface area of boundary between two adjacent cells (m^2)

d = distance between cell centers (m)

$$dSO4Red = RedRate * \text{matrix cell volume} * dT \qquad (2.2)$$

dSO4Red = amount of SO_4^{2-} reduced to S^{2-} during a dT (mol)

RedRate = rate of SO_4^{2-} reduction to S^{2-} (mol m^{-3} s^{-1})

Matrix cell volume (m^3)

dT (s)

A schematic description of the program is shown in Figure 2-8 and all intermediary results were collected in a folder on the computer for possible further study. Example images of the distributions of $^{35}SO_4^{2-}$ and $^{35}S^{2-}$ at three different times across a cross section marked with a dashed line in Figure 2-7 can be found in Appendix A.2.

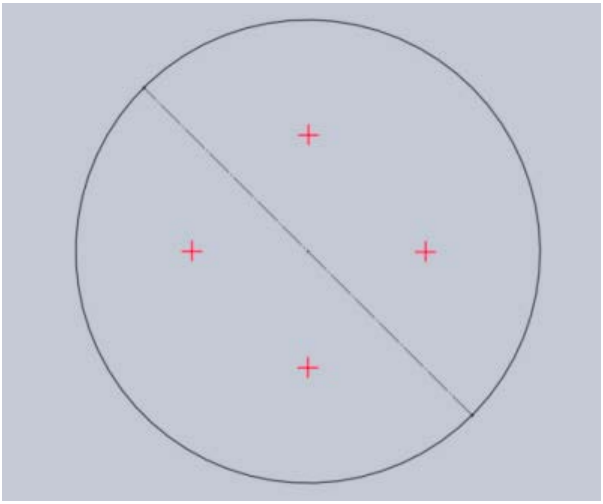

Figure 2-7. *Top view of a model test cell where + signs show the positions for addition of $^{35}SO_4^{2-}$, SO_4^{2-} and lactate.*

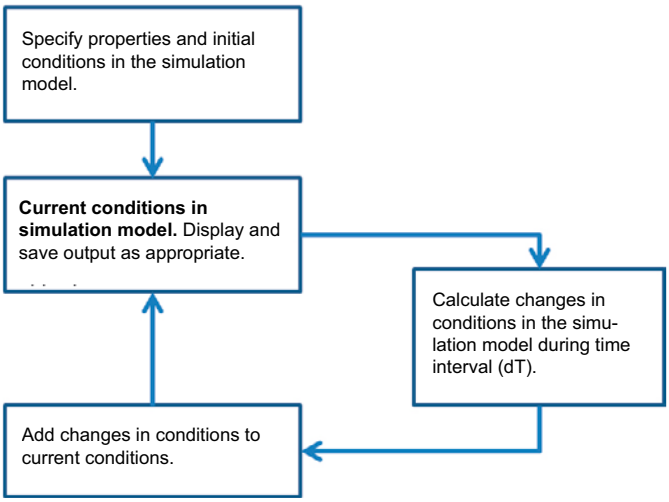

Figure 2-8. *A schematic illustration of the simulation program.*

2.8.3 Sensitivity analysis

To determine the impact of the uncertainties in diffusion coefficients for SO_4^{2-} and S^{2-} through the clay cores on the results, some extra runs of the evaluation program was run. These runs all concern test cell 8 and were all run with identical input data except for the values of the diffusion coefficients.

2.9 Data processing, graphics and statistics

Data processing, statistical analyses and data visualizations were performed using Microsoft Office Excel 2010 (Microsoft Corporation, Redmond, USA) and Statsoft Statistica 64 (Statsoft, Tulsa, USA) software.

3 Results

Detailed tables of results are given in Appendix A.3.

3.1 Copper discs

Radioactivity in the form of $Cu_x{}^{35}S$ accumulated on the discs (Figure 3-1 and Figure 3-2) was converted to Becquerel (Bq) (= disintegrations per second (dps)). Results were adjusted for half-life of the isotope, instrument efficiency (2%) and background radiation (Table 3-1). Immediately when the test cells were opened an obvious difference between the 1,750 kg m^{-3} and the 2,000 kg m^{-3} discs was observed. All the 1,750 kg m^{-3} discs had black precipitates on the surface while the 2,000 kg m^{-3} discs were clean from black precipitates. When analysed in the autoradiograph, on average, a 10,000 times higher surface radioactivity was measured on the (+) 1,750 kg m^{-3} discs compared to the (+) 2,000 kg/m^3 discs (Table 3-1). Heat treatment of the clay did not have any significant sterilization effect in the 1,750 kg m^{-3} cells that showed similar levels of radioactivity on the disks compared to the discs in 1,750 kg m^{-3} cells with added SRB. This means that the SRB residing in the commercial clay survived heat treatment.

In the 2,000 kg m^{-3} case the cells with added microbes showed a low level of sulphide-producing activity and the heat treated cells did not show any measurable radioactivity on their discs. The cells with added microbes showed small spots of $Cu_x{}^{35}S$ mostly on the edges of the discs (Figure 3-2). These spots were probably formed by germinating spore forming SRB that took advantage of heterogeneities in the clay or roughness of the copper discs. Furthermore, the thin boundary space between the test cell inner wall and the edge of the clay core might not have reached up to full swelling pressure. This could explain why Cu_xS mostly was formed on the edges of these discs. In the centre were the density reached 2,000 kg m^{-3} only a few small radioactive spots were found. This demonstrates how extremely important the swelling pressure is for bacterial sulphide-producing activity in compacted clays.

Back-calculations for half-life of the isotope, instrument efficiency (2%) and background radiation were done as follows:

$$Bq = 1/2\text{^}((-t/T½)/\left(\frac{Counts_{gross}-Counts_{blank}}{Time_{measurement}}\right) * Instrument\ efficiency) \quad (3.1)$$

Bq = disintegrations per second (dps)

t = time (days) since manufacturing of isotope (start of half-life)

T½ = half-life of isotope (87.4 days)

$Counts_{gross}$ = raw counts from radioactive copper disc

$Counts_{blank}$ = raw counts from non-radioactive copper disc

$Time_{measurement}$ = measurement time (1,800 seconds)

Instrument efficiency = 2%

The total amount of S on the copper discs was calculated as follows:

$$Total\ S = \frac{N(t)}{N_{added}} * Added\ 35_{SO4^{2-}} * Isotope\ dilution \quad (3.2)$$

N(t) = the quantity (Bq) that still remains and has not yet decayed after a time, *t* (days)

N_{added} = specific activity isotope (55.28 TBq/mmol)*$Added\ 35_{SO4^{2-}}$ (mol)

$Added\ 35_{SO4^{2-}}$ (mol) = Added volume isotope (L)*Isotope concentration (M)

Isotope dilution = $\frac{\text{pore water volume (L)*concentration of leachable } SO_4{}^{2-}\text{(M)}}{Added\ 35_{SO4^{2-}}\ \text{(mol)}}$

Table 3-1. Radioactivity detected on the copper discs, recalculated for isotope dilutions and half-life of the isotope.

Test cell code	Surface activity (KBq)	Total amount of S (µmole)
T3 1750 (+) 47d	1,598	26
T4 1750 (+) 77d	1,586	26
T5 1750 (+) 123d	528	9
T1 1750 (−) 123d	593	9
T2 1750 (−) 123d	1,126	17
T8 2000 (+) 47d	0.2	0.01
T9 2000 (+) 77d	0.1	0.002
T10 2000 (+) 123d	0.6	0.02
T6 2000 (−) 123d	0.0001	< 0.000003
T7 2000 (−) 123d	0.0001	< 0.000003

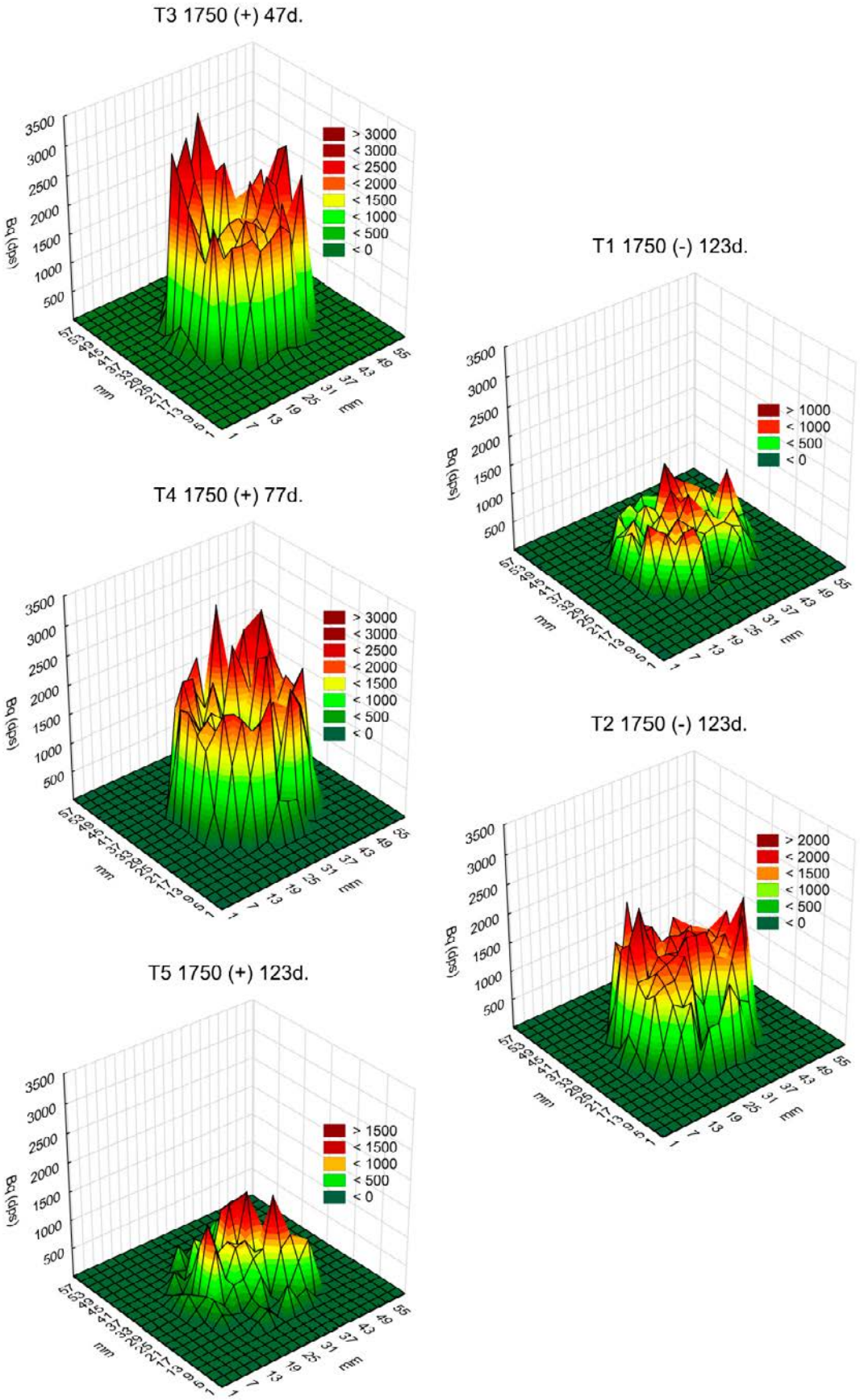

Figure 3-1. *3D raw data plots from autoradiography analysis of copper discs for test cells 1–5. T = Test cell, 1,750 or 2,000 = 1,750 or 2,000 kg m^{-3}, (+/–) = with/without added microbes, d = days of incubation. Color scale according to legend for each image. Counts are adjusted for half-life of the isotope (87.4 days).*

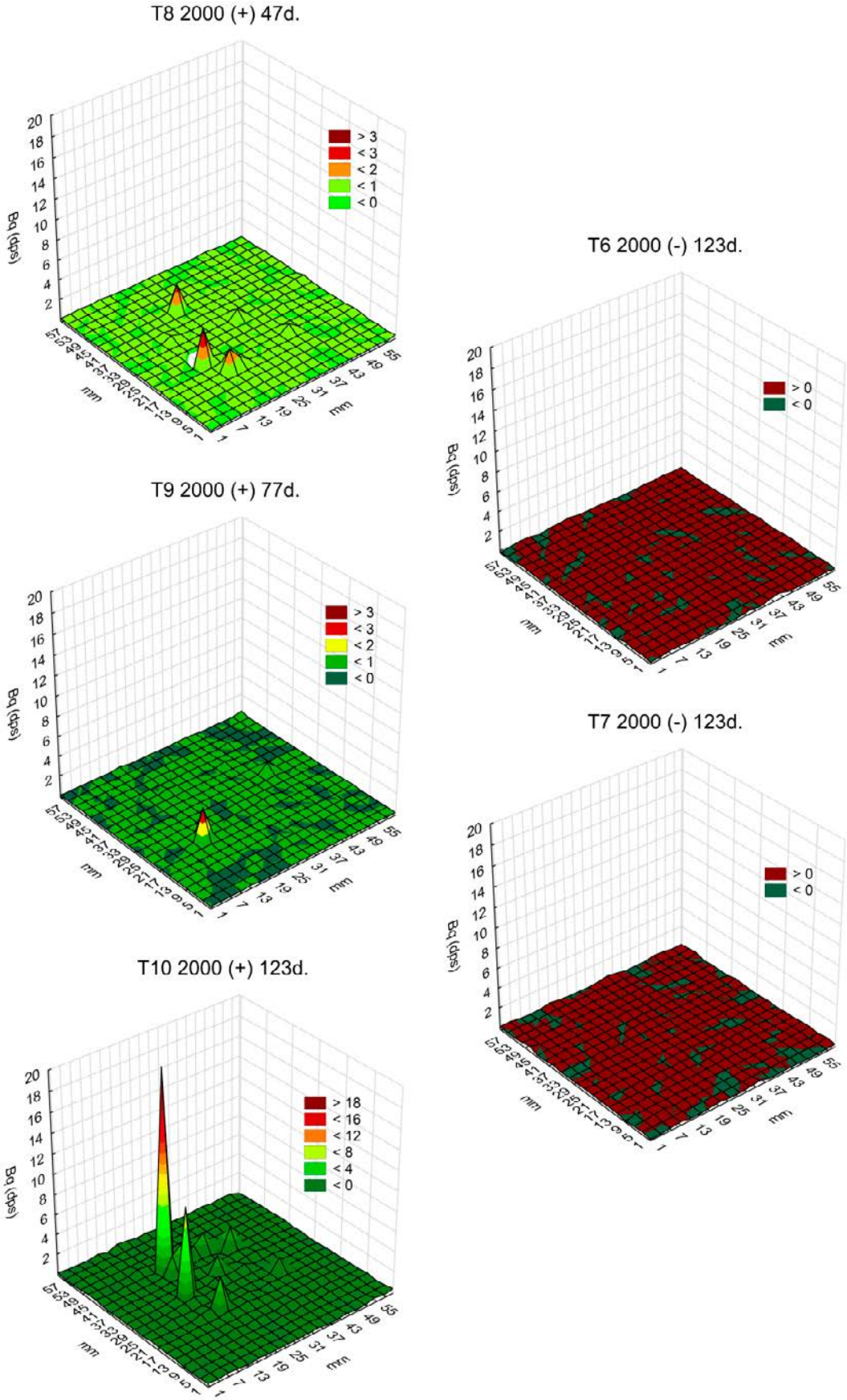

Figure 3-2. *3D raw data plots from autoradiography analysis of copper discs for test cells 6–10 T = Test cell, 1,750 or 2,000 = 1,750 or 2,000 kg m^{-3}, (+/−) = with/without added microbes, d = days of incubation. Color scale according to legend for each image. Counts are adjusted for half-life of the isotope (87.4 days).*

3.2 MPN-samples

The MPN results demonstrate how well the SRB community in the clay survived during incubation. Results from MPN analysis match results from radioactivity measurement on the copper discs to some extent. In the 1,750 cases (added microbes or not) an increasing trend over time was found, with relatively high bacterial numbers from the latest sampling at 123 days compared to day 47 (Table 3-2). For the 2,000 case, low numbers of cultivable SRB were found in the test cells with added microbes and the numbers were below detection in the heat treated clay cells without addition of microbes, consistent with the radioactivity measurement on the copper discs from these test cells. Overall the viable SRB seem to be evenly distributed through the clay core since similar numbers were found in all three positions for each test cell, except for some of the 1,750 cells where higher numbers were found in the top and bottom position compared to the middle (Table 3-2).

Table 3-2. Most probable numbers of SRB in the clay cores. Sample positions are shown in Figure 2-6.

	Position					
	Bottom (closest to copper) (MPN $L^{-1} \cdot 10^6$)		Middle (MPN $L^{-1} \cdot 10^6$)		Top (MPN $L^{-1} \cdot 10^6$)	
Test cell code		Lower-upper 95% confidence interval		Lower-upper 95% confidence interval		Lower-upper 95% confidence interval
T3 1750 (+) 47d	> 20	–	> 21	–	> 20	–
T4 1750 (+) 77d	28	13–74	16	6–49	18	8–46
T5 1750 (+) 123d	> 189	–	112	37–360	170	64–563
T1 1750 (−) 123d	> 201	–	< 0.2	–	1	0.5–3
T2 1750 (−) 123d	> 201	–	6	2–21	170	64–563
T8 2000 (+) 47d	0.6	0.2–1	0.4	0.2–1	5	2–13
T9 2000 (+) 77d	0.4	0.2–1	0.1	0.04–0.4	0.3	0.1–0.7
T10 2000 (+) 123d	0.2	0.1–0.6	0.4	0.2–1	0.2	0.1–0.6
T6 2000 (−) 123d	< 0.04	–	< 0.04	–	< 0.04	–
T7 2000 (−) 123d	< 0.04	–	< 0.04	–	< 0.04	–

3.3 Distribution of ^{35}S in the clay core

In Table 3-3 the amount of added $^{35}SO_4^{2-}$ at the start of the experiment to each test cell is compared to the average measured ^{35}S at the end from three positions (test cell 3 and 8) or six layers (remaining test cells) in Bq L^{-1}. Results were adjusted for half-life of the ^{35}S isotope and the scintillation instrument efficiency (36%). The results show that with the uncertainty of the analysis, meaning instrument efficiency etc., basically all of the added ^{35}S in the form of $^{35}SO_4^{2-}$ could be accounted for at the end of the experiments. The analysis method does not separate $^{35}SO_4$ from ^{35}S in the clay pore water. The graphs in Figure 3-3 and the numbers in Table 3-3 should not be interpreted in detail because of uncertainties such as measurement errors, but the trend where the first millimetre close to the 1,750 kg m^{-3} coppers discs contained more ^{35}S than the rest of the clay core is, however, quite clear.

3.4 Distribution of SO_4^{2-} in the clay core

The average amount of SO_4^{2-} in raw, dry bentonite clay was determined to 22 µmoles g^{-1} (SD ±0.89 µmoles g^{-1}). This amount was obtained for all five dilutions from 10 to 50 mL, i.e. the amount of leachable SO_4^{2-} was independent of the volume used to disperse the bentonite clay. A second batch of water did not result in more SO_4^{2-}, all SO_4^{2-} was leached in the first round. The leaching experiment demonstrated that there was an easily dissolved fraction of SO_4^{2-} in the MX-80 bentonite clay used for the experiments presented in this report. The amount of 22 µmoles g^{-1}

corresponds to 0.07% by weight of S in the bentonite clay which corresponds reasonably well with the amount of S-SO_4 of 0.13% determined in bentonite clay from the canister retrieval experiment using evolved gas analysis (Dueck et al. 2011).

The average calculated concentration of SO_4^{2-} in the clay core exceeded the added non-radioactive SO_4^{2-} 500–1,000 times (Table 3-4). The addition of approximately 0.1 mM extra SO_4^{2-} was obviously not needed; the clay pore water contained far more SO_4^{2-} than this and much more than what is found in groundwater, i.e. 1–5 mM. The average concentration of SO_4^{2-} analysed after the experiments was approximately 50% of the concentration obtained by leaching of raw, not compacted bentonite clay. However, it was found that the distribution of this SO_4^{2-} was uneven with low concentrations close to the copper surface for many of the test cells (Figure 3-4). This uneven distribution was most pronounced for the 2,000 kg m^{-3} test cells and the shortest incubation times. It appears likely that the addition of water saturation medium (Table 2-2) to the clay from the copper disc side of the test cells washed out SO_4^{2-} from the first 5 mm of the clay core towards the middle of the core. This redistribution of SO_4^{2-} was probably most effective at start of water saturation before swelling reduced water transport from a mass transport to a diffusion transport. Over time, SO_4^{2-} appeared to have diffused back to the wash out zone, and this process was fastest in the low density test cells.

Table 3-3. Average concentrations of ^{35}S in pore water in the clay cores.

Test cell code	Added ^{35}S (nM)	Average measured ^{35}S (nM)	Ratio (measured/ added)
T3 1750 (+) 47d	58	81	1.40
T4 1750 (+) 77d	58	113	1.96
T5 1750 (+) 123d	58	99	1.71
T1 1750 (−) 123d	59	164	2.75
T2 1750 (−) 123d	59	125	2.11
T8 2000 (+) 47d	56	137	2.45
T9 2000 (+) 77d	56	157	2.82
T10 2000 (+) 123d	56	144	2.59
T6 2000 (−) 123d	59	143	2.42
T7 2000 (−) 123d	59	159	2.69

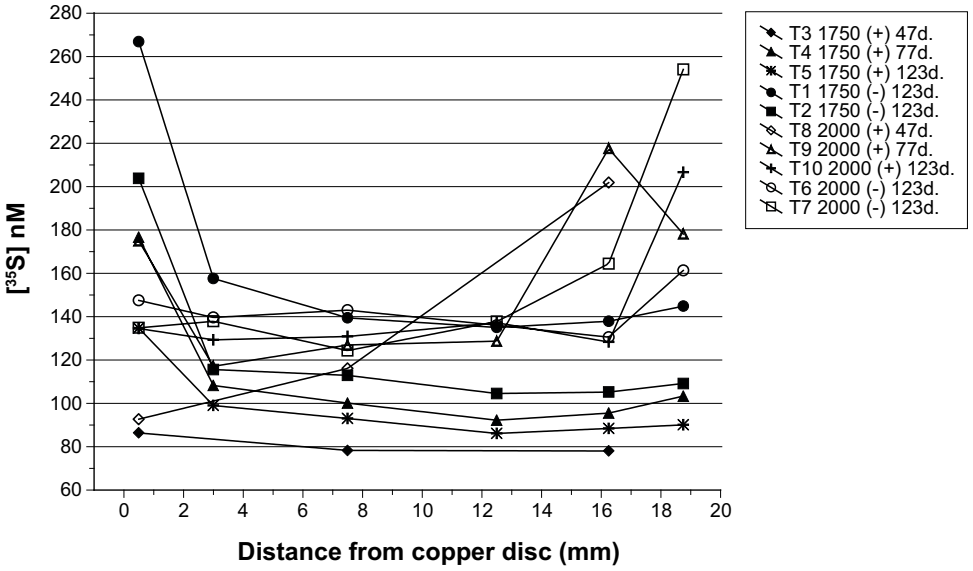

Figure 3-3. *Concentrations of ^{35}S in profiles in the clay core for each test cell. Test cell number, clay density, addition of microbes (+/−) and incubation time according to legend.*

Table 3-4. Average concentrations of added and leachable SO_4^{2-} in the clay cores at start of the experiments and the concentrations analysed at end of the experiments.

Test cell code	Added SO_4^{2-} (mM)	SO_4^{2-} leachable from the clay (mM)	Average analysed SO_4^{2-} in the clay cores (mM)
T3 1750 (+) 47d	0.12	55	11
T4 1750 (+) 77d	0.12	55	34
T5 1750 (+) 123d	0.12	55	36
T1 1750 (−) 123d	0.13	54	50
T2 1750 (−) 123d	0.13	54	42
T8 2000 (+) 47d	0.12	128	70
T9 2000 (+) 77d	0.12	128	81
T10 2000 (+) 123d	0.12	128	80
T6 2000 (−) 123d	0.13	125	67
T7 2000 (−) 123d	0.13	125	68

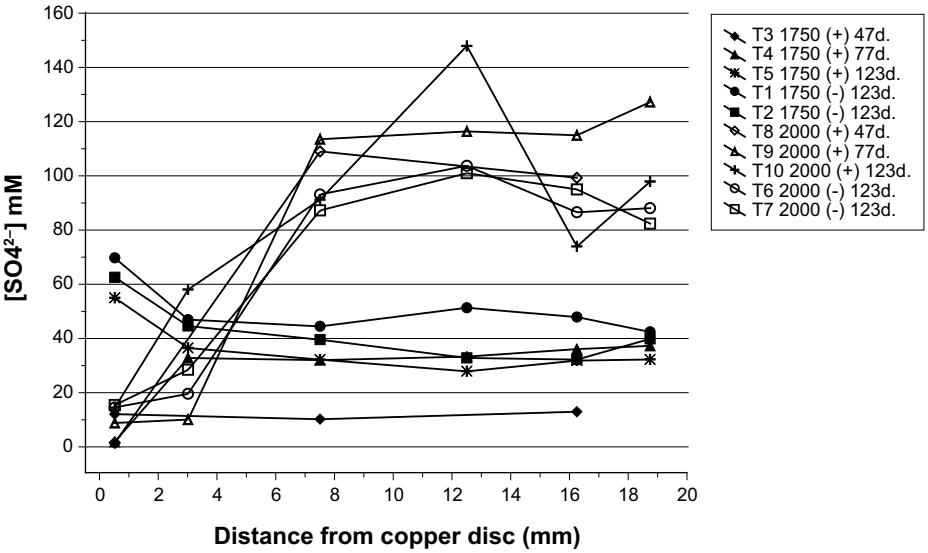

Figure 3-4. *Concentrations of SO_4^{2-} in profiles of the clay core for each test cell. Test cell number, clay density, addition of microbes (+/−) and incubation time according to legend.*

3.5 Rate of SO_4^{2-} to S^{2-} reduction

The finite difference method used in the computer program that derived the SO_4^{2-} to S^{2-} reduction rate can be used to do so with arbitrary numerical accuracy. Using a short time interval (dT) and dividing the test cell into many cells gives high accuracy. As dT approaches zero and the number of cells approaches infinity the numerical accuracy approaches perfection. The price paid for this increase in accuracy is greater need for computing power and time. The choices of dT and the numbers of cells used to compute the results in Table 3-5 have been made so that the numerical accuracy of the calculations are at least an order of magnitude better than the uncertainty of the input data into the program. This is obvious when comparing the results for the same input data run with dT= 900 instead of 600 and 31×31×31 cells instead of 51×51×51. This was done as part of the sensitivity analysis for test cell 8 and the difference in result was minor, i.e. $6.2 \cdot 10^{-9}$ (Table 3-5) and $6.3 \cdot 10^{-9}$ (Table 3-6), respectively. The sensitivity analysis demonstrated that increasing the diffusion coefficient for S^{2-} 3 orders of magnitude resulted in a 20 times decrease in the calculated reduction rate (Table 3-6) while a 3 orders of magnitude increase of the diffusion coefficient for SO_4^{2-} returned a 7 times decrease in the reduction rate. The calculated rates were consequently 3 times more sensitive to the choice of diffusion coefficient for S^{2-} than for SO_4^{2-}.

The implications of the calculated reduction rates are further treated in the discussion, section 4.4.

Table 3-5. SO_4^{2-} and S^{2-} diffusion coefficients and SO_4^{2-} to S^{2-} reduction rates for all test cells. For test cell 6 and 7 where no activity could be detected on the copper discs the detection limit for reduction rates are based on an imaginary value of 1 gross count.

Test cell code	Diffusion coefficient SO_4^{2-} ($m^2\ s^{-1}$)	Diffusion coefficient S^{2-} ($m^2\ s^{-1}$)	dT (s)	SO_4^{2-} to S^{2-} reduction rate (mol $s^{-1}\ m^{-3}$)
T3 1750 (+) 47d	$1.2\cdot10^{-11}$	$2.4\cdot10^{-11}$	300	$9.8\cdot10^{-7}$
T4 1750 (+) 77d	$1.2\cdot10^{-11}$	$2.4\cdot10^{-11}$	300	$3.9\cdot10^{-7}$
T5 1750 (+) 123d	$1.2\cdot10^{-11}$	$2.4\cdot10^{-11}$	300	$6.0\cdot10^{-8}$
T1 1750 (−) 123d	$1.2\cdot10^{-11}$	$2.4\cdot10^{-11}$	300	$6.6\cdot10^{-8}$
T2 1750 (−) 123d	$1.2\cdot10^{-11}$	$2.4\cdot10^{-11}$	300	$1.2\cdot10^{-7}$
T8 2000 (+) 47d	$2.0\cdot10^{-12}$	$4.0\cdot10^{-12}$	600	$9.5\cdot10^{-9}$
T9 2000 (+) 77d	$2.0\cdot10^{-12}$	$4.0\cdot10^{-12}$	600	$1.4\cdot10^{-10}$
T10 2000 (+) 123d	$2.0\cdot10^{-12}$	$4.0\cdot10^{-12}$	600	$5.0\cdot10^{-10}$
T6 2000 (−) 123d	$2.0\cdot10^{-12}$	$4.0\cdot10^{-12}$	600	$< 5.7\cdot10^{-14}$
T7 2000 (−) 123d	$2.0\cdot10^{-12}$	$4.0\cdot10^{-12}$	600	$< 5.7\cdot10^{-14}$

Table 3-6. Sensitivity analysis for variation of diffusion coefficients for SO_4^{2-} and S^{2-} on the calculated SO_4^{2-} to S^{2-} reduction rate (mole $s^{-1}\ m^{-3}$) applied on test cell 8. The used values and the resulting rate for the used coefficients in Table 3-5 is marked in blue.

Diffusion coefficient SO_4^{2-} ($m^2\ s^{-1}$)	Diffusion coefficient S^{2-} ($m^2\ s^{-1}$)					
	$1\cdot10^{-10}$	**$2\cdot10^{-11}$**	**$1\cdot10^{-11}$**	**$4\cdot10^{-12}$**	**$2\cdot10^{-12}$**	**$4\cdot10^{-13}$**
$1\cdot10^{-10}$	$9.6\cdot10^{-11}$		$2.9\cdot10^{-10}$		$6.8\cdot10^{-10}$	$1.6\cdot10^{-7}$
$2\cdot10^{-11}$			$3.0\cdot10^{-10}$		$7.4\cdot10^{-10}$	$2.1\cdot10^{-9}$
$1\cdot10^{-11}$	$9.9\cdot10^{-11}$	$2.2\cdot10^{-10}$		$5.6\cdot10^{-10}$		
$4\cdot10^{-12}$			$4.3\cdot10^{-10}$		$1.4\cdot10^{-9}$	$5.6\cdot10^{-9}$
$2\cdot10^{-12}$	$1.5\cdot10^{-10}$	$5.0\cdot10^{-10}$		$9.5\cdot10^{-9}$		
$4\cdot10^{-13}$	$6.8\cdot10^{-10}$	$7.1\cdot10^{-9}$		$2.1\cdot10^{-5}$		

4 Discussion

4.1 Experimental set-up

The experimental set-up was developed based on experiences from previous experiments using test cells made of stainless steel (Pedersen et al. 2000b, Pedersen 2010, Masurat et al. 2010b). The test cells used in this experiment were made of titanium because this metal does not easily react with S^{2-} (Persson et al. 2011), which may be the case with stainless steel. Further, in earlier experiments, it was found that microbial S^{2-}-producing activity in free water adjacent to the clay cores became very intensive and the produced S^{2-} interfered with the analysis of the S^{2-} production rates inside the clay cores (Pedersen 2010). Therefore, the present experimental equipment was constructed to exclude any free water in contact with the clay cores after the addition of carbon sources and $^{35}SO_4^{2-}$. Any production of $^{35}S^{2-}$ in the present experiments must have originated from bacterial SO_4^{2-}-reducing activity inside the clay cores.

The present set-up employed copper discs installed at one end of the clay core which differs from the preceding experiment where 1.6 cm^2 copper test plates (1×5×13 mm) were positioned in depth profiles of the clay core (Masurat et al. 2010b, Pedersen 2010). The present configuration was a return to an older configuration where silver foils were installed at the end of the core (Pedersen et al. 2000b). The use of one large metal surface of 9.6 cm^2 compared to 4 smaller surfaces ($4 \times 1.6 = 6.4$ cm^2) was reasonably comparable with respect to the surface area. Both configurations will report similar total amounts of $^{35}S^{2-}$. However, the configuration with a bottom metal plate can be argued to more appropriately simulate a buffer-copper-canister interface.

The knowledge of a strong relation between the density of the clay and survival and activity of microorganisms in compacted MX-80 bentonite clay was established a long time ago (Motamedi et al. 1996). It is likely that the swelling pressure has an important role in the control of microbial activity in compacted bentonite clay. The wet density and the corresponding swelling pressure of a compacted clay core is determined by compaction space, amount of bentonite clay and water saturation. Previously, swelling pressure was set by water saturation of clays at different densities in test cells. In the present experiment, the test cells were installed with force transducers that precisely reported swelling pressures throughout the experiments and confirmed that the expected swelling pressures were achieved.

The radioactive isotope ^{35}S was used as a tracer for microbial sulphide-producing activity in these experiments. Because this isotope has a short half-life of only 87.4 days it constitutes a very sensitive tracer for microbial sulphide-production. This isotope has, therefore, been successfully used for studies of microbial sulphide-production in marine sediments for several decades (Jørgensen 1978). From stable isotope studies, in pure cultures and in the field, it has been found that the light isotope, $^{32}SO_4^{2-}$ is metabolized faster than $^{35}SO_4^{2-}$. The relative discrimination against $^{35}SO_4^{2-}$ will depend on the species of SRB present, growth conditions and available substrates (Brüchert et al. 2001). Typically, the fractionation factor, α, can be 1.05–1.06 (Rudnicki et al. 2001). The enrichment factor, ε, vary similarly depending on the concentrations of $^{32}SO_4^{2-}$ and $^{35}SO_4^{2-}$ at start and end of a growth period if the system is closed without an external supply of SO_4^{2-} (Detmers et al. 2001). The fractionation factor was not known for the SRB populations under the conditions they encountered in the studied clay cores. Therefore, the data were not compensated for a possible fractionation of $^{32}SO_4^{2-}/^{35}SO_4^{2-}$ which means that the modelled rates may have been underestimated by a couple of percent. However, this work was designed to compare microbial sulphide-producing activity under varying wet densities and swelling pressures which were the only variables applied. All other conditions, concentrations of electron donors, acceptors, temperature and carbon sources were kept constant. A similar α factor can therefore safely be anticipated for all test cells and comparisons of microbial activity over density and pressure will be valid.

4.2 Distribution of $^{35}SO_4^{2-}$ and SO_4^{2-} in the clay

At start of the experiment, 0.06 µM $^{35}SO_4^{2-}$ was added together with approximately 0.1 mM SO_4^{2-} on top of the clay cores (Table 2-1 and Figure 2-7). The extra SO_4^{2-} was added to dilute the isotope and ensure that it diffused readily and did not precipitate at the points of addition. The carbon source was lactate that was added to a final pore water concentration of 28 mM. Because the clay naturally contained 55–125 mM leachable SO_4^{2-} (Table 3-4), there was enough of this electron acceptor to allow complete bacterial oxidation of the lactate with $^{35}SO_4^{2-}/SO_4^{2-}$. The concentrations of leachable SO_4^{2-} and analyzed SO_4^{2-} in the pore water agrees well with concentrations of approximately 100 mM calculated for pore water in compacted MX-80 bentonite clay (Bradbury and Baeyens 2003).

The results showed an un-even distribution of SO_4^{2-} over depth in the clay core that was most pronounced in the high 2,000 kg m^{-3} test cells and at the shortest incubation times (Figure 3-4). This was most likely due to redistribution of leachable SO_4^{2-} during the re-saturation phase that was occurring from the core front via a titanium filter, later in the experiments replaced by the copper disc. The re-distribution effect was mitigated over time and was not visible in the 1,750 kg m^{-3} test cells after 47 d but was visible in the 2,000 kg m^{-3} test cells throughout the experiment. However, the distribution of $^{35}SO_4^{2-}$ by diffusion was not influenced. The concentration of $^{35}SO_4^{2-}$ rapidly diffused and resulted in an even distribution in the 1,750 kg m^{-3} test cells while, as expected, the diffusion of $^{35}SO_4^{2-}$ was slower in the 2,000 kg m^{-3} test cells.

Species susceptible to redistribution are mainly ions affecting hydration of montmorillonite and thus swelling and hydraulic conductivity and this redistribution, therefore, introduce several uncertainties for the results on S^{2-} producing rates, in particular for the 2,000 kg m^{-3} test cells. Firstly, the compensation for dilution of the isotope by naturally occurring SO_4^{2-} was done based on an average distribution. Because there was less SO_4^{2-} analysed in the 1 mm of the core closest to the copper disc and more at 5 mm distance compared to what was assumed, the rates may have been partly overestimated close to the copper discs and underestimated in the remaining part of the for the 2,000 kg m^{-3} clay cores. We keep these rates because these divergences from the perfect SO_4^{2-} distribution case equalize reasonably well as the sum of SO_4^{2-} was known and used in the calculations. Secondly, the redistribution was not only valid for SO_4^{2-}, it must also be valid for all ions leachable with water such as Na^+ and Cl^-, to retain charge balance in the pore water. This may in turn have influenced the swelling pressure in the washed out zone of the clay, i.e. there may have been a more or less pronounced skewed distribution of swelling pressure in the clay, despite the fact the total pressure of the clay was reported by the force transducers exactly as planned (Figure 2-4). There are several ways around this problem in the future. The most obvious would be to prolong the water saturation phase long enough to allow the redistribution to be mitigated by diffusion but that may take very long time. A second possibility can be to increase the concentration of SO_4^{2-} in the saturation medium to a concentration between half to equal of the leachable SO_4^{2-} concentration. Thirdly, saturation medium addition can be done on the core side opposite to the copper disc; the redistribution will remain, but the effect will simulate a water saturation scenario of buffer around a copper canister in the small scale.

4.3 Survival and cultivability of sulphate-reducing bacteria

The presence of viable bacteria and SRB in commercial bentonite clays has been demonstrated previously (Masurat et al. 2010a, Svensson et al. 2011). In an earlier experiment, heat treatment at 120°C for 15 h failed to kill indigenous bacteria in the clay (Masurat et al. 2010b). The present heat treatment of the clay at 110°C for 170 h intended to sterilize the clay from bacteria, prolonged exposure to heat was expected to be efficient. Obviously this was still not enough to kill off SRB in the clay because intensive sulphide-producing activity and large numbers of cultivable SRB were observed in the 1,750 kg m^{-3} test cells with heat treated clay (Table 3-2 and Table 3-5) but not in the 2,000 kg m^{-3} test cells with heat treated clay. It should be noted that the heat treated clay was not added with SRB. Previously, it has repeatedly been shown that viability of bacteria in compacted bentonite clay is negatively correlated with increasing density and swelling pressure (Motamedi et al. 1996, Pedersen et al. 2000a). The present results corroborate this correlation where the numbers of SRB were approximately 1,000 times larger in the 1,750 kg m^{-3} test cells compared to

the 2,000 kg m^{-3} test cells. It was also found that the combination of heat treatment and a high density reduced numbers of cultivable SRB and their activity to numbers below detection. Based on previous and present results, it appears safe to conclude that microbial survival and sulphide-producing activity is strongly reduced, or even inhibited, when the density related swelling pressure approaches 5 MPa. The precise cut-off density remains to determine as does the issue on how microorganisms in highly compacted bentonite clay react if the swelling pressure is decreased, for instance by so called bentonite clay erosion (Birgersson et al. 2009) or by contact with high salinity groundwater. It is also unknown if all previous and present density related effects on microbial activity are specific for MX-80, or if the relation between density and microbial activity varies with the type of bentonite clay at similar densities and/or swelling pressures.

4.4 Determination of sulphide production rates

The output from modelling of bacterial sulphide-production rates in the clay cores depends on the choice of diffusion coefficients. There was some uncertainty about the values for SO_4^{2-} and S^{2-} because the literature is fairly short on such values, particularly for S^{2-} while some values can be found for SO_4^{2-}. In a work investigating gypsum dissolution, the actual/apparent diffusion coefficient for SO_4^{2-} in a sodium Wyoming bentonite clay (dry density 1,460 kg m^{-3}) was determined to $4.2 \cdot 10^{-12}$ m^2 s^{-1} (Birgersson et al. 2009). The calculated value for diffusion coefficient for SO_4^{2-} in FEBEX bentonite clay (dry density 1,650 kg m^{-3}) was also $4.2 \cdot 10^{-12}$ m^2 s^{-1} (García-Gutiérrez et al. 2006). Previously, we calculated diffusion coefficients for S^{2-} in compacted Wyoming MX-80 bentonite clay based on the transport of S^{2-} from sulphide-production activity to known S^{2-}concentrations in water outside the clay (Pedersen 2010). The coefficient for S^{2-} in Wyoming MX-80 at a wet density of 2,000 kg m^{-3} became $2 \cdot 10^{-12}$ m^2 s^{-1} which is approximately 50% slower than the rate used in this work for clay cores at a wet density of 2,000 kg m^{-3}. A relation between the wet density and the rate of diffusion was determined to be linear at $0.4 \cdot 10^{-11}$ units per 100 kg m^{-3} wet density (approximately 75 kg m^{-3} dry density). This relation was used for both the SO_4^{2-} and the S^{2-} diffusion coefficients starting with a coefficient of $2 \cdot 10^{-12}$ m^2 s^{-1} for SO_4^{2-} at a wet density of 2,000 kg m^{-3} and a dry density of 1,600 kg m^{-3}. That number compare well with the number of $4.2 \cdot 10^{-12}$ m^2 s^{-1} at a dry density of 1,460 kg m^{-3} taking the relation between density and rate into consideration, although an exact match may not apply due to different experimental configurations. Further, it was assumed that S^{2-} diffused with a rate that was twice that of SO_4^{2-}. The smaller diffusion coefficient, the faster sulphide-producing activity must be modelled in the clay to obtain the observed radioactivity on the copper surfaces as demonstrated by the sensitivity analysis results (Table 3-6). The diffusion coefficients used to produce the modelling results in Table 4-1 are probably in the lower regime of what can be assumed correct, thereby giving the modelling results conservative values.

The rate of $SO_4^{2-}$to S^{2-} reduction decreased over incubation time for both test densities (Table 3-5). There can be several reasons for this result. Firstly, if the numbers of viable SRB decreased over time, the corresponding sulphide-producing activity would decrease. However, the cultivation results do not show any significant decrease in numbers of SRB over time, except for one position in the 2,000 kg m^{-3} case (Table 3-2). Secondly, the redistribution of SO_4^{2-} may have decreased the isotope dilution factor significantly. This could occur if the $^{35}SO_4^{2-}$ diffused faster towards the copper surface than the relocated SO_4^{2-} did, something that is indicated by the analysis results in Figure 3-3 and Figure 3-4. That would produce more $^{35}S^{2-}$ close to the copper surface than what was calculated with the expected isotopic dilution. Over time, when redistributed SO_4^{2-} has equalized again in the clay, this effect will diminish. The distribution data of SO_4^{2-} indicate that the equalization of SO_4^{2-} concentrations in the clay occurred after 47 days in the 1,750 kg m^{-3} case and was still ongoing in the 2,000 kg m^{-3} case after 123 days (Figure 3-4). Lastly, we did observe an increase in ^{35}S close to the copper surfaces for both cases except for the 47 days samples. This effect was very clear in the 1,750 kg m^{-3} cases but less obvious for the 2,000 kg m^{-3} cases. It may consequently be that some of the produced S^{2-} did not stay on, or reached, the copper discs but was located in the clay close to the copper discs, which indeed had a black appearance nearby to the copper discs in the 1,750 kg m^{-3} test cells, in particular for the 77 and 123 days cases. That would have underestimated the S^{2-} production because it was only ^{35}S on the copper discs that were accounted for in the modelling. If this was the case, the modelling will predict a lower S^{2-} production rate in the clay than what was actually the case.

In a previous experiment with SRB in the water outside the clay and addition of lactate, S^{2-} was detected in a range from 1 to $650 \cdot 10^{-9}$ moles of S^{2-} per test plate (Pedersen 2010). Here, the range was 4 to 22,000 moles of S^{2-} per test disc (Table 3-1). The test plates had a surface of 0.65 cm^2 while the discs had a surface of 9.6 cm^2 which means that there is a factor of 15 that must be taken into consideration before a comparison is done. If the test discs are normalized to the plates, the range becomes 0.3 to $1{,}470 \cdot 10^{-9}$ moles of S^{2-} per test plate. In other words, the amounts of S^{2-} that reached the copper surfaces in the previous experiments and the experiments presented here are comparable in range.

4.5 Sulphide production rates in relation to the long-term disposal of spent nuclear fuel

There are four stoichiometric compounds of copper sulphides: chalcocite (Cu_2S), digenite ($Cu_{1.8}S$), djurleite ($Cu_{1.96}S$), and anilite ($Cu_{1.75}S$). The copper canister in the high level waste repository is proposed to be 50 mm thick. Assuming only chalcocite is produced and that the corrosion of the copper canister is constant in space and time, a maximum S^{2-}-production rate can be calculated using Eqs. (4.1) and (4.2) that would allow integrity of the canister for the planned lifespan of the repository.

The chemical reaction for forming chalcocite is:

$$2Cu(s) + H_2S \Rightarrow Cu_2S(s) + H_{2(g)} \quad (4.1)$$

and the maximum corrosion rate can be expressed as:

$$corr_{max} = \frac{d*copper}{2*M}\frac{1}{t} \quad (4.2)$$

where $corr_{max}$ is the maximum corrosion rate limiting the copper canister integrity over the repository lifetime, d is the density of copper ($8.96 \cdot 10^{-3}$g mm^{-3}), copper is the thickness of the copper canister wall (50 mm), M is the molar mass of copper (63.546 g mol^{-1}), and t is the duration of spent nuclear fuel disposal; here we use $3.65 \cdot 10^7$ days. Eq. (4.2) gives a maximum S^{2-} corrosion rate of 4,000 fmol h^{-1} mm^{-2} H_2S for the canister to remain intact for 100,000 years ($3.65 \cdot 10^7$ days) and 400 fmol h^{-1} mm^{-2} H_2S for the canister to remain intact for 1,000,000 year.

Comparing the calculated $corr_{max}$ above with the results in Table 4-1 gives mean S^{2-} corrosion rates much higher than $corr_{max}$ for 1,750 kg m^{-3} and close to the $corr_{max}$ for 2,000 kg m^{-3}. The only test cells that pass the requirement are the sterile 2,000 kg m^{-3} test cells and test cell T9.

The results of a previous investigation and calculation of rates were based on the available SO_4^{2-} in the test cells originating solely from the added groundwater and the added radioactive labelled SO_4^{2-} (Pedersen 2010). If the leachable gypsum in the bentonite clay had been included as a source of SO_4^{2-}, the calculated mean S^{2-} production rates would have been 10 to 100 times higher which must be kept in mind when comparing the results from that work with the present work.

Table 4-1. Reduction rates of SO_4^{2-} to S^{2-} from Table 3-5 to rates per mm^3 and per mm^2 under a clay column of 350 mm length.

Test cell code	SO_4^{2-} to S^{2-} reduction rate (mol s^{-1} m^{-3})	SO_4^{2-} to S^{2-} reduction rate (mol h^{-1} mm^{-3})	SO_4^{2-} to S^{2-} reduction rate (mol h^{-1} mm^{-2})
T3 1750 (+) 47d	$9.8 \cdot 10^{-7}$	$3.5 \cdot 10^{-12}$	$1{,}100{,}000 \cdot 10^{-15}$
T4 1750 (+) 77d	$3.9 \cdot 10^{-7}$	$1.4 \cdot 10^{-12}$	$420{,}000 \cdot 10^{-15}$
T5 1750 (+) 123d	$6.0 \cdot 10^{-8}$	$2.2 \cdot 10^{-13}$	$65{,}000 \cdot 10^{-15}$
T1 1750 (−) 123d	$6.6 \cdot 10^{-8}$	$2.4 \cdot 10^{-13}$	$71{,}000 \cdot 10^{-15}$
T2 1750 (−) 123d	$1.2 \cdot 10^{-7}$	$4.5 \cdot 10^{-13}$	$130{,}000 \cdot 10^{-15}$
T8 2000 (+) 47d	$9.5 \cdot 10^{-9}$	$3.4 \cdot 10^{-14}$	$10{,}000 \cdot 10^{-15}$
T9 2000 (+) 77d	$1.4 \cdot 10^{-10}$	$5.1 \cdot 10^{-16}$	$150 \cdot 10^{-15}$
T10 2000 (+) 123d	$5.0 \cdot 10^{-10}$	$1.8 \cdot 10^{-15}$	$540 \cdot 10^{-15}$
T6 2000 (−) 123d	$< 5.7 \cdot 10^{-14}$	$< 2.1 \cdot 10^{-19}$	$< 0.06 \cdot 10^{-15}$
T7 2000 (−) 123d	$< 5.7 \cdot 10^{-14}$	$< 2.1 \cdot 10^{-19}$	$< 0.06 \cdot 10^{-15}$

5 Conclusions

The improvement to exclude a free aqueous phase outside the clay core in this experiment led to that all of the sulphide-producing activity took place inside the clay where it was intended. The experimental setup was to have a high sensitivity which was accomplished. However, this also led to that the activity in the 1,750 kg m^{-3} test cells practically was above our detection range. This will however not be an issue in future experiments where the lowest density will be higher than 1,750 kg m^{-3}.

The uneven SO_4^{2-} distribution that occurred in the 2,000 kg m^{-3} test cells (discussed in 4.2) created uncertainties for the S^{2-} production rates. In future experiments we suggest that saturation medium addition should be done on the core side opposite to the copper disc. The redistribution will remain, but the effect will simulate a water saturation scenario of buffer around a copper canister in the small scale.

All together this experiment shows that the seemingly small change in density from 1,750 to 2,000 kg m^{-3} makes a huge difference for opportunistic bacteria such as SRB when all other variables are kept favourable for microbial activity. A variable that was not introduced in this study is temperature. In a high level radioactive waste repository the heat generated from the decay of the radioactive waste will raise temperatures close to the canister up to approximately 90°C. In future experiments could microbial activity as a function of temperature easily be tested by simultaneously incubating the test cells in a heating cabinet at varying temperatures.

It is also still uncertain if other types of bentonite clay (e.g. Asha or Calcigel) will have the same effects on microbial activity at similar densities and/or swelling pressures, since all previous and present density related effects on microbial activity in bentonite clay has mainly been studied for MX-80.

6 References

SKB's (Svensk Kärnbränslehantering AB) publications can be found at www.skb.se/publications.

Birgersson M, Börgesson L, Hedström M, Karnland O, Nilsson U, 2009. Bentonite erosion. Final report. SKB TR-09-34, Svensk Kärnbränslehantering AB.

Bradbury M H, Baeyens B, 2003. Porewater chemistry in compacted re-saturated MX-80 bentonite. Journal of Contaminant Hydrology 61, 329–338.

Brüchert V, Knoblauch C, Jørgensen B B, 2001. Controls on stable sulfur isotope fractionation during bacterial sulfate reduction in Arctic sediments. Geochimica et Cosmochimica Acta 65, 763–776.

Coulson J M, Richardson J F, 1990. Chemical engineering. 4th ed. Vol. 1. Oxford: Pergamon.

Detmers J V, Brüchert K, Habicht S, Kuever J, 2001. Diversity of sulfur isotope fractionations by sulfate-reducing prokaryotes. Applied and Environmental Microbiology 67, 888–894.

Dueck A, Johannesson L-E, Kristensson O, Olsson S, 2011. Report on hydro-mechanical and chemical-mineralogical analyses of the bentonite buffer in Canister Retrieval Test. SKB TR-11-07, Svensk Kärnbränslehantering AB.

García-Gutiérrez M, Cormenzana J L, Missana T, Mingarro M, Molinero J, 2006. Overview of laboratory methods employed for obtaining diffusion coefficients in FEBEX compacted bentonite. Journal of Iberian Geology 32, 37–53.

Greenberg A E, Clesceri L S, Eaton A D, 1992. Estimation of bacterial density. In Standard methods for the examination of water and wastewater. 18th ed. Washington: American Public Health Association, 9–49.

Hallbeck L, 2014. Determination of sulphide production rates in laboratory cultures of the sulphate reducing bacterium *Desulfovibrio aespoeensi*s with lactate and H_2 as energy sources. SKB TR-14-14, Svensk Kärnbränslehantering AB.

Hallbeck L, Pedersen K, 2008. Characterization of microbial processes in deep aquifers of the Fennoscandian Shield. Applied Geochemistry 23, 1796–1819.

Hobbie J E, Daley R J, Jasper S, 1977. Use of nucleopore filters for counting bacteria by fluorescence microscopy. Applied and Environmental Microbiology 33, 1225–1228.

Jørgensen, B B, 1978. A comparison of methods for the quantification of bacterial sulfate reduction in coastal marine sediments. I. Measurement with radiotracer techniques. Geomicrobiology Journal 1, 11–27.

Masurat P, Eriksson S, Pedersen K, 2010a. Evidence of indigenous sulphate-reducing bacteria in commercial Wyoming bentonite MX-80. Applied Clay Science 47, 51–57.

Masurat P, Eriksson S, Pedersen K, 2010b. Microbial sulphide production in compacted Wyoming bentonite MX-80 under in situ conditions relevant to a repository for high-level radioactive waste. Applied Clay Science 47, 58–64.

Morton K W, Mayers D F, 2005. Numerical solution of partial differential equations: an introduction. 2nd ed. Cambridge: Cambridge University Press, 151–193.

Motamedi M, 1999. The survival and activity of bacteria in compacted bentonite clay in conditions relevant to high level radioactive waste (HLW) repositories. PhD thesis. Göteborg University, Göteborg, 1–45.

Motamedi M, Pedersen K, 1998. *Desulfovibrio aespoeensis* sp nov., a mesophilic sulfate-reducing bacterium from deep groundwater at Äspö hard rock laboratory, Sweden. International Journal of Systematic Bacteriology 48, 311–315.

Motamedi M, Karland O, Pedersen K, 1996. Survial of sulfate reducing bacteria at different water activities in compacted bentonite. FEMS Microbiology Letters 141, 83–87.

Pedersen K, 2010. Analysis of copper corrosion in compacted bentonite clay as a function of clay density and growth conditions for sulphate-reducing bacteria. Journal of Applied Microbiology 108, 1094–1104.

Pedersen K, 2012a. Subterranean microbial populations metabolize hydrogen and acetate under in situ conditions in granitic groundwater at 450 m depth in the Äspö Hard Rock Laboratory, Sweden. FEMS Microbiology Ecology 81, 217–229.

Pedersen K, 2012b. Influence of H_2 and O_2 on sulphate-reducing activity of a subterranean community and the coupled response in redox potential. FEMS Microbiology Ecology 82, 653–665.

Pedersen K, Ekendahl S, 1990. Distribution and activity of bacteria in deep granitic groundwaters of southeastern Sweden. Microbial Ecology 20, 37–52.

Pedersen K, Motamedi M, Karnland O, Sandén T, 2000a. Cultivability of microorganisms introduced into a compacted bentonite clay buffer under high-level radioactive waste repository conditions. Engineering Geology 58, 149–161.

Pedersen K, Motamedi M, Karnland O, Sandén T, 2000b. Mixing and sulphate-reducing activity of bacteria in swelling compacted bentonite clay under high-level radioactive waste repository conditions. Journal of Applied Microbiology 89, 1038–1047.

Persson J, Lydmark S, Edlund J, Pääjärvi A, Pedersen K, 2011. Microbial incidence on copper and titanium embedded in compacted bentonite clay. SKB R-11-22, Svensk Kärnbränslehantering AB.

Rudnicki, M, Elderfield H, Spiro B, 2001. Fractionation of sulfur isotopes during bacterial sulfate reduction in deep ocean sediments at elevated temperatures. Geochimica et Cosmochimica Acta 65, 777–789.

Stroes-Gascoyne S, Pedersen K, Haveman S A, Dekeyser K, Arlinger J, Daumas S, Ekendahl S, Hallbeck L, Hamon C J, Jahromi N, Delaney T-L, 1997. Occurrence and identification of microorganisms in compacted clay-based buffer material designed for use in a nuclear fuel waste disposal vault. Canadian Journal of Microbiology 43, 1133–1146.

Svensson D, Dueck A, Nilsson U, Sandén T, Lydmark S, Jägevall S, Pedersen K, Hansen S, 2011. Alternative buffer material. Status of the ongoing investigation of reference materials and test package 1. SKB TR-11-06, Svensk Kärnbränslehantering AB.

Widdel F, Bak F, 1992. Gram-negative, mesophilic sulphate-reducing bacteria. In Balows A, Trüper H G, Dworkin M, Harder W, Schleifer K-Z (eds). The prokaryotes. Vol 4. New York: Springer, 3352–3378.

Appendix A

A.1 Pressures in test cells

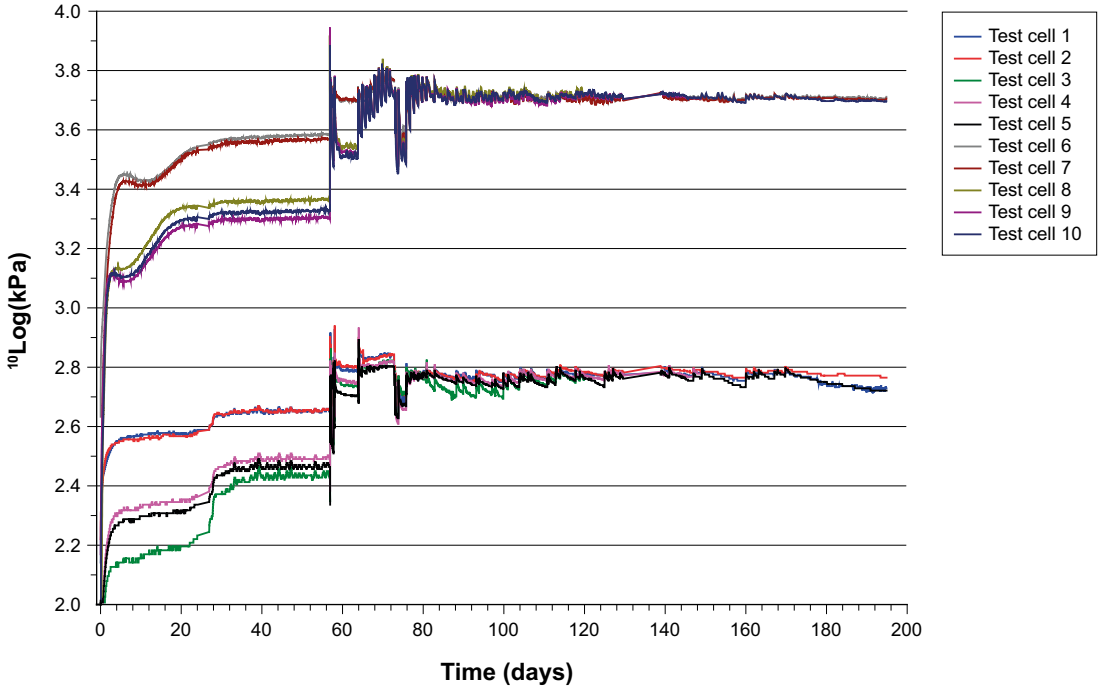

Figure A-1. *Pressures in test cells according to legend. 1–5 = 1,750 kg m^{-3}. 6–10 = 2,000 kg m^{-3}.*

A.2 Modelling sulphate diffusion

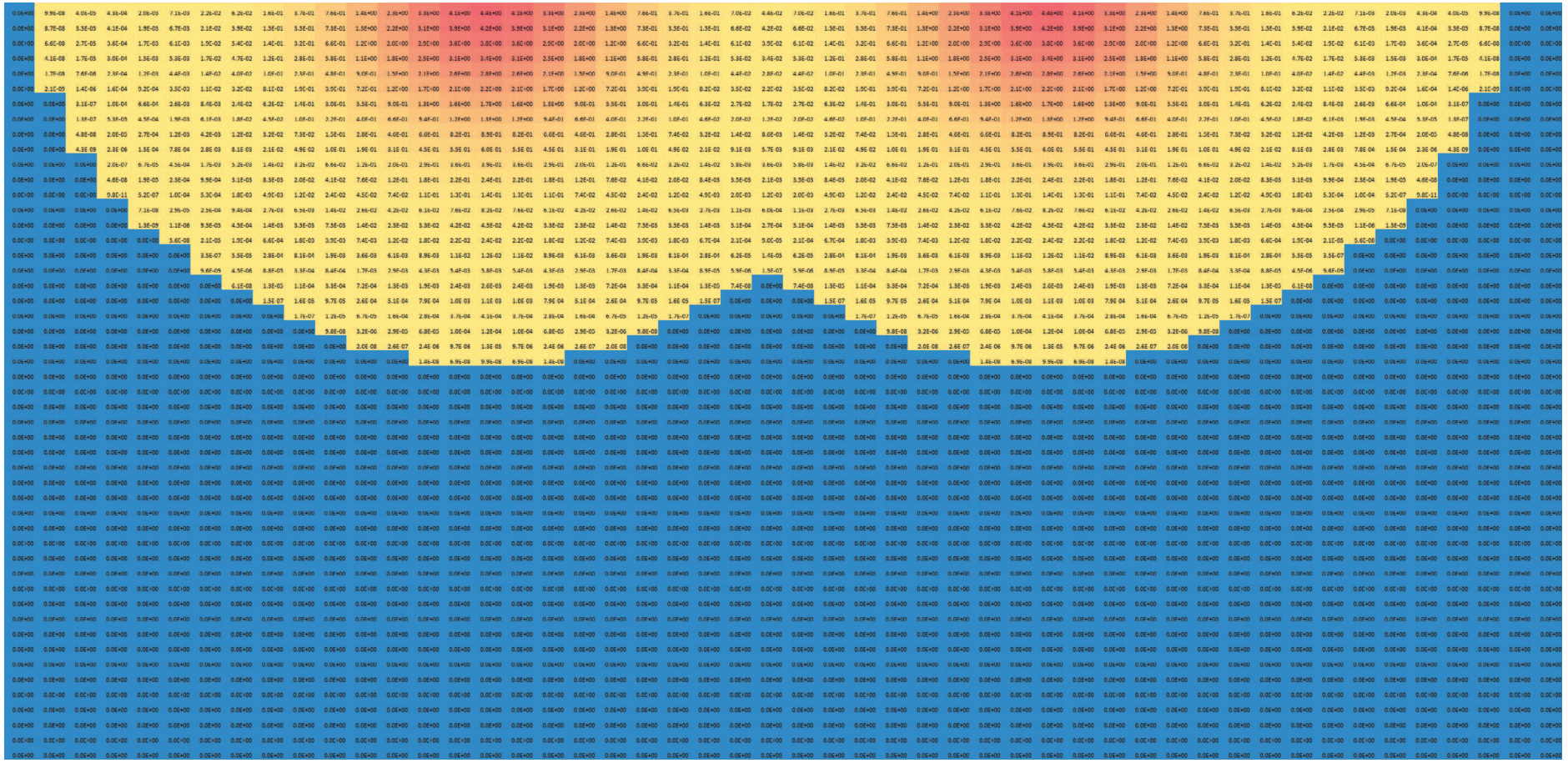

Figure A-2. *$^{35}SO_4^{2-}$ distribution at time T=10 days in T8 2000 (+) 47d.·10^{-15} (mol·m^{-3}).*

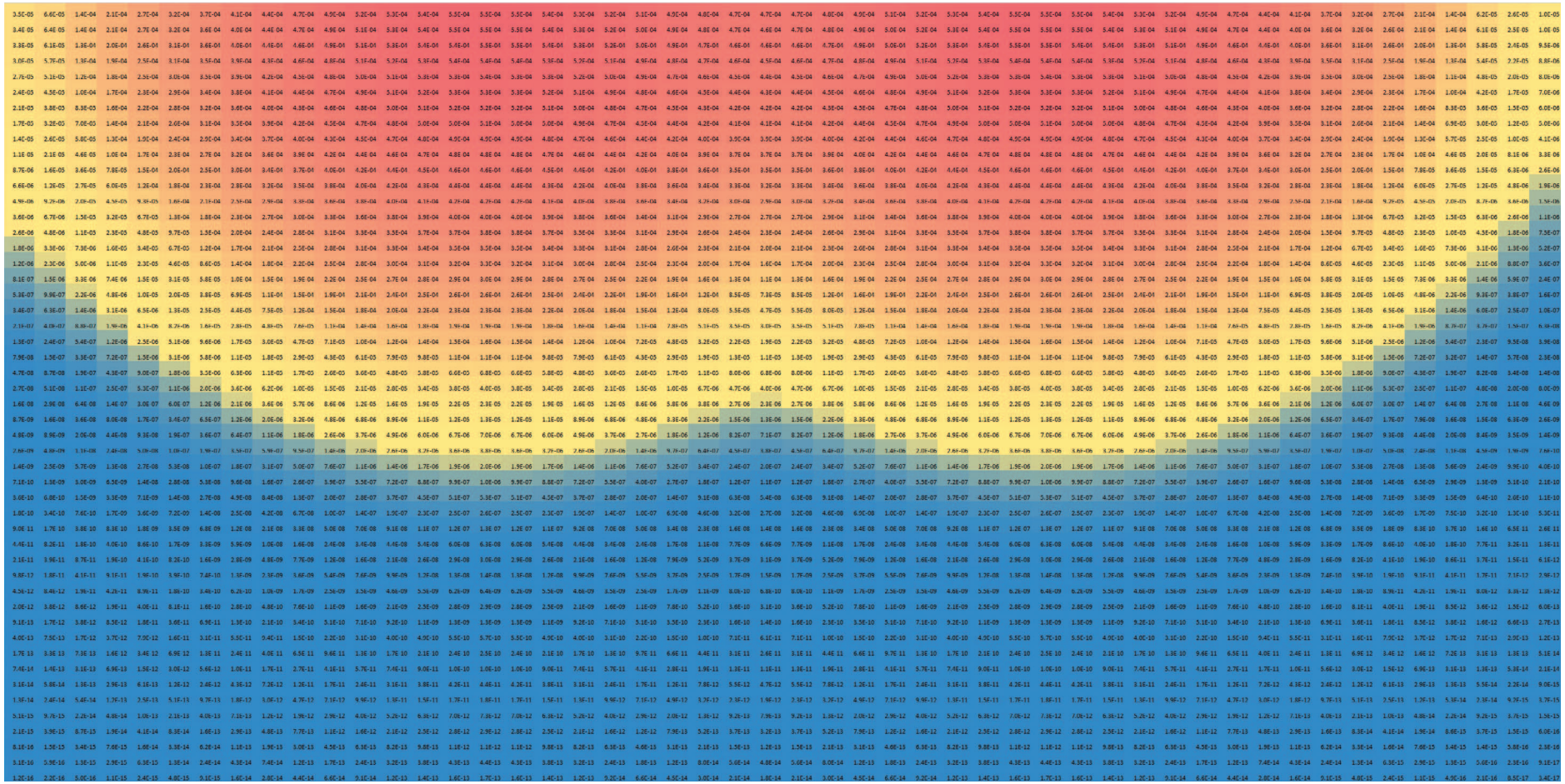

Figure A-3. *$^{35}S^{2-}$ distribution at time T=10 days in T8 2000 (+) 47d.·10^{-15} (mol·m^{-3}).*

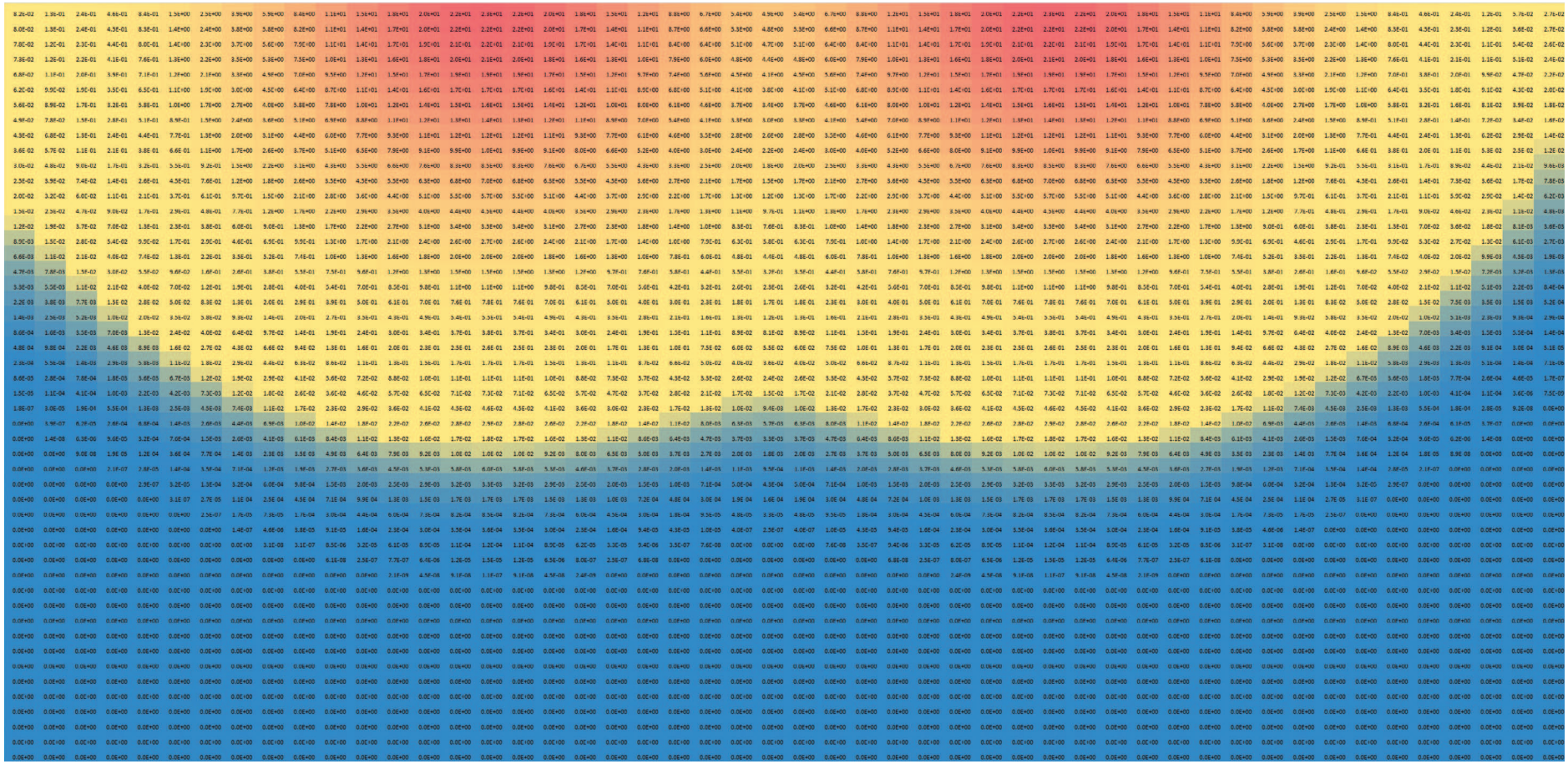

Figure A-4. *$^{35}SO_4^{2-}$ distribution at time T=25 days in T8 2000 (+) 47d.·10^{-15} (mol·m^{-3}).*

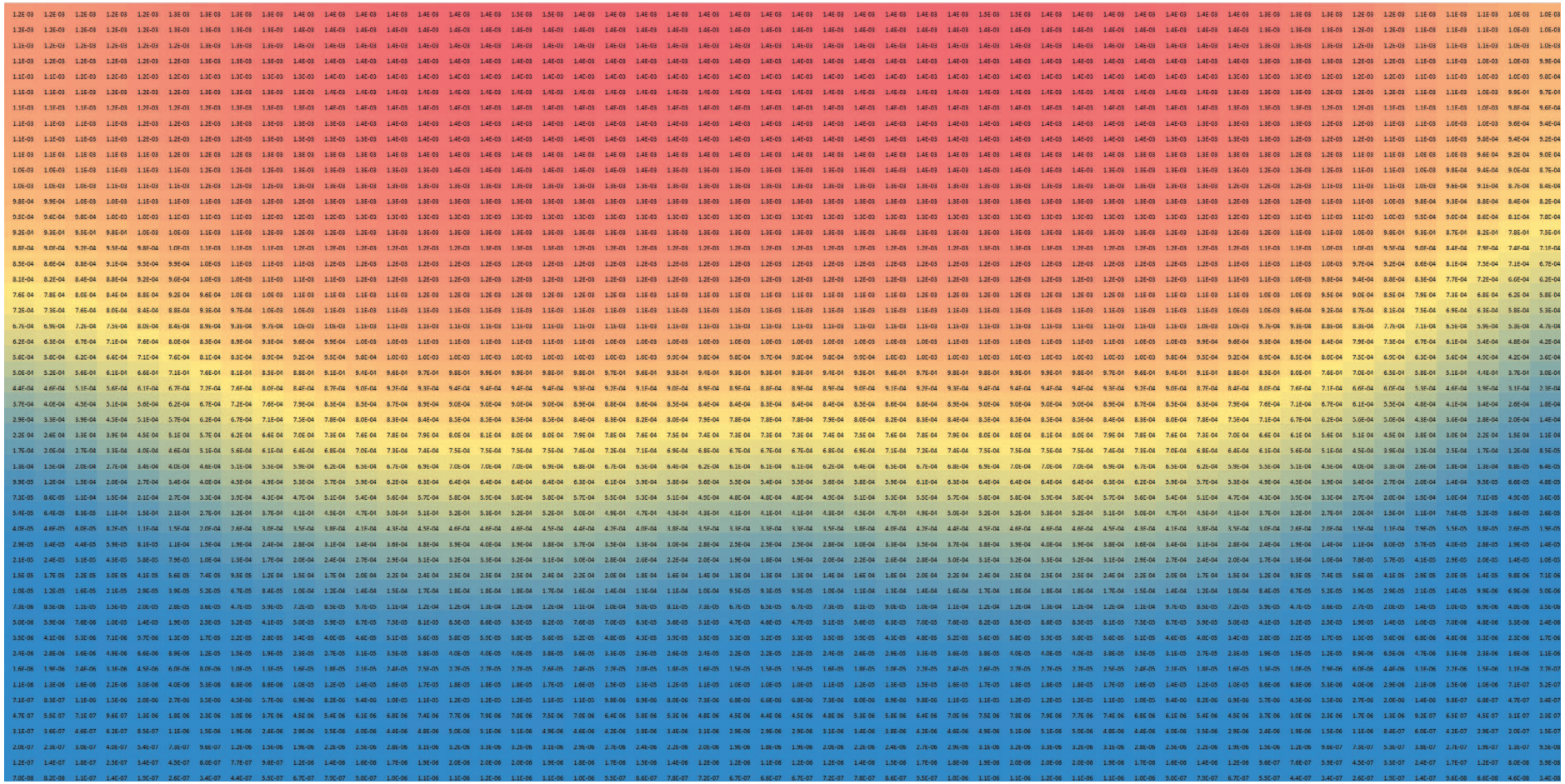

Figure A-5. *$^{35}S^{2-}$ distribution at time T=25 days in T8 2000 (+) 47d.·10^{-15} (mol·m^{-3}).*

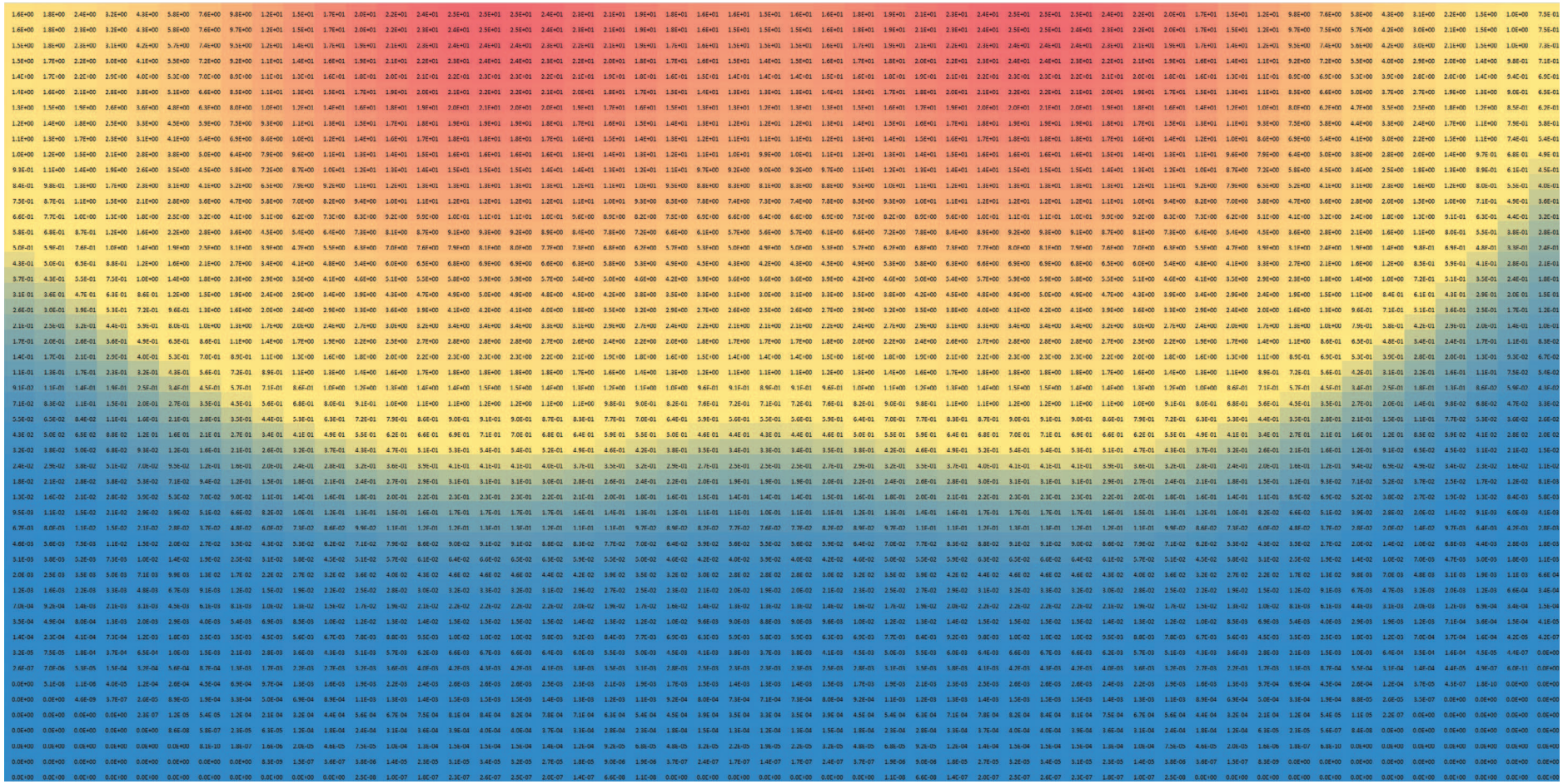

Figure A-6. *$^{35}SO_4^{2-}$ distribution at time T=47 days in T8 2000 (+) 47d.·10^{-15} (mol·m^{-3}).*

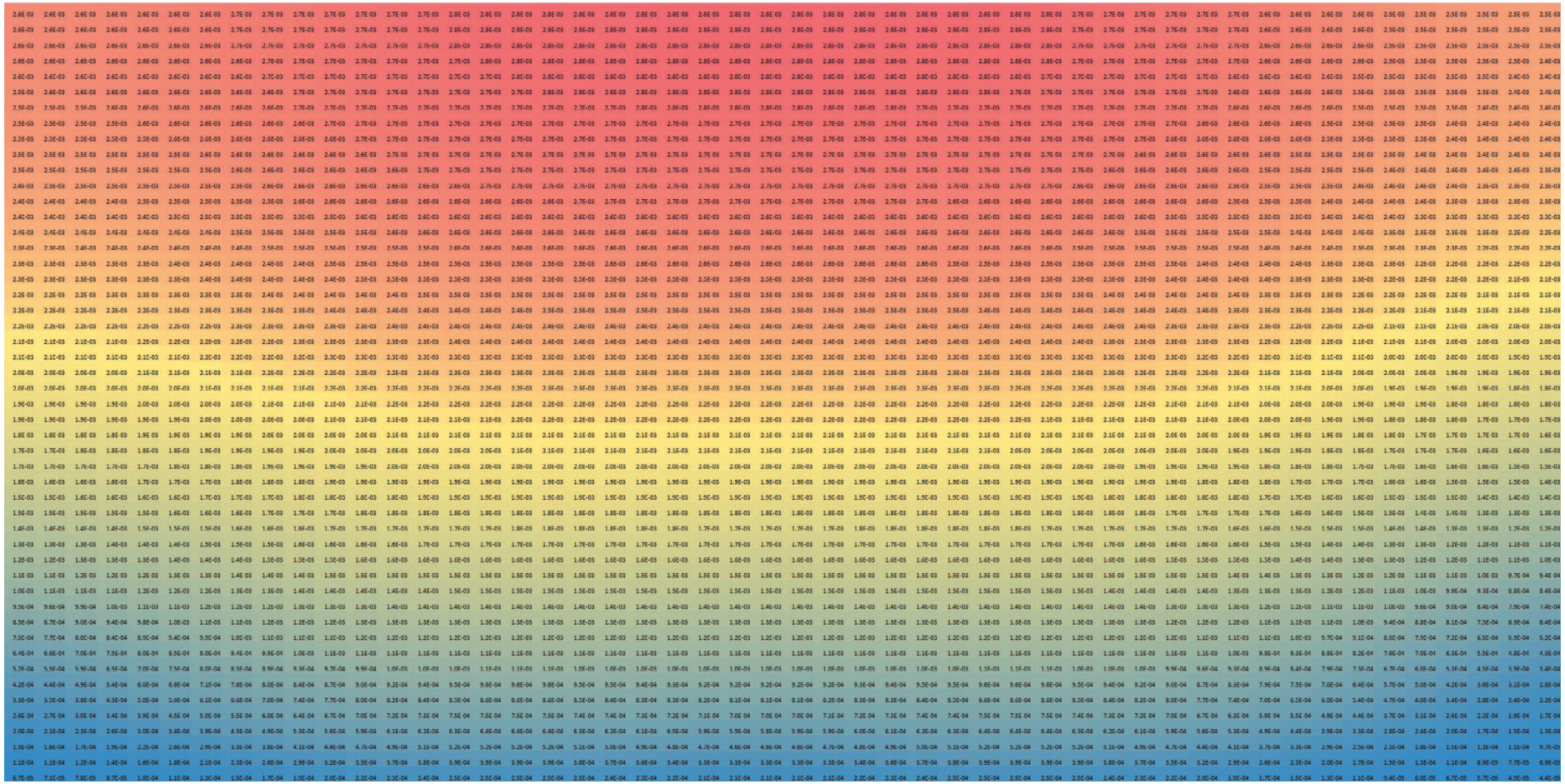

Figure A-7. *$^{35}S^{2-}$ distribution at time T=47 days in T8 2000 (+) 47d.·10^{-15} (mol·m^{-3}).*

A.3 ^{35}S measurements on copper discs

Test cell code	Gross counts adjusted for blank (counts)	Measurement time (s)	Counts per second (cps)	Instrument efficiency (%)	Disintegrations per second (dps) (Bq)	Time elapsed since isotope preparation (days)	Half-life ^{35}S (days)	Normalized activity (dps) (Bq)
T3 1750 (+) 47d	2.77E+07	1,800	1.54E+04	2	7.71E+05	92	87.4	1.60E+06
T4 1750 (+) 77d	2.77E+07	1,800	1.54E+04	2	7.71E+05	91	87.4	1.59E+06
T5 1750 (+) 123d	6.52E+06	1,800	3.62E+03	2	1.81E+05	135	87.4	5.28E+05
T1 1750 (−) 123d	7.31E+06	1,800	4.06E+03	2	2.03E+05	135	87.4	5.93E+05
T2 1750 (−) 123d	1.39E+07	1,800	7.72E+03	2	3.86E+05	135	87.4	1.13E+06
T8 2000 (+) 47d	2.78E+03	1,800	1.54E+00	2	7.72E+01	92	87.4	1.60E+02
T9 2000 (+) 77d	1.03E+03	1,800	5.72E–01	2	2.86E+01	91	87.4	5.89E+01
T10 2000 (+) 123d	6.81E+03	1,800	3.78E+00	2	1.89E+02	135	87.4	5.52E+02
T6 2000 (−) 123d	1.00E+00	1,800	5.56E–04	2	2.78E–02	135	87.4	< 1
T7 2000 (−) 123d	1.00E+00	1,800	5.56E–04	2	2.78E–02	135	87.4	< 1

A.4 ^{35}S measurements in clay cores

Test cell code	Clay fraction	Counts per minute (cpm)	Instrument efficiency (%)	Disintegrations per second (dps)	Time elapsed since isotope preparation (days)	Half-life ^{35}S (days)	Normalized activity (dps) (Bq)	Amount ^{35}S (mmole)	Pore water volume (L)	Amount ^{35}S per liter (mM)	Average amount ^{35}S per liter (mM)
T3 1750 (+) 47d											
	Sample 1, pos. 1	5.36E+04	36	9.93E+05	64	87.4	1.65E+06	3.37E–08	0.00039	8.71E–05	
	Sample 2, pos. 1	4.66E+04	36	8.62E+05	64	87.4	1.43E+06	2.92E–08	0.00034	8.56E–05	8.63E–05
	Sample 1, pos. 2	3.68E+04	36	6.82E+05	64	87.4	1.13E+06	2.31E–08	0.00032	7.17E–05	
	Sample 2, pos. 2	4.32E+04	36	8.00E+05	64	87.4	1.33E+06	2.71E–08	0.00032	8.49E–05	7.83E–05
	Sample 1, pos. 3	2.84E+04	36	5.27E+05	64	87.4	8.75E+05	1.79E–08	0.00032	5.54E–05	
	Sample 2, pos. 3	5.43E+04	36	1.01E+06	64	87.4	1.67E+06	3.41E–08	0.00034	1.01E–04	7.80E–05
T4 1750 (+) 77d											
	0–1 mm	6.18E+04	36	1.14E+06	102	87.4	2.57E+06	5.24E–08	0.00030	1.77E–04	
	1–5 mm	2.23E+05	36	4.13E+06	102	87.4	9.28E+06	1.89E–07	0.00175	1.08E–04	
	5–10 mm	1.77E+05	36	3.29E+06	102	87.4	7.38E+06	1.51E–07	0.00150	1.00E–04	
	10–15 mm	2.12E+05	36	3.93E+06	102	87.4	8.82E+06	1.80E–07	0.00195	9.22E–05	
	15–17.5 mm	1.16E+05	36	2.14E+06	102	87.4	4.81E+06	9.82E–08	0.00103	9.55E–05	
	17.5–20 mm	1.71E+05	36	3.16E+06	102	87.4	7.10E+06	1.45E–07	0.00140	1.03E–04	1.13E–04

Test cell code	Clay fraction	Counts per minute (cpm)	Instrument efficiency (%)	Disintegrations per second (dps)	Time elapsed since isotope preparation (days)	Half-life ^{35}S (days)	Normalized activity (dps) (Bq)	Amount ^{35}S (mmole)	Pore water volume (L)	Amount ^{35}S per liter (mM)	Average amount ^{35}S per liter (mM)
T5 1750 (+) 123d											
	0–1 mm	1.56E+04	36	2.89E+05	144	87.4	9.06E+05	1.85E–08	0.0001	1.35E–04	
	1–5 mm	1.64E+05	36	3.04E+06	144	87.4	9.53E+06	1.94E–07	0.0020	9.90E–05	
	5–10 mm	1.34E+05	36	2.48E+06	144	87.4	7.77E+06	1.59E–07	0.0017	9.30E–05	
	10–15 mm	1.22E+05	36	2.25E+06	144	87.4	7.05E+06	1.44E–07	0.0017	8.61E–05	
	15–17.5 mm	1.09E+05	36	2.02E+06	144	87.4	6.32E+06	1.29E–07	0.0015	8.84E–05	
	17.5–20 mm	7.97E+04	36	1.48E+06	144	87.4	4.62E+06	9.43E–08	0.0010	9.01E–05	9.85E–05
T1 1750 (–) 123d											
	0–1 mm	1.62E+04	36	3.01E+05	144	87.4	9.43E+05	1.92E–08	0.0001	2.67E–04	
	1–5 mm	3.10E+05	36	5.74E+06	144	87.4	1.80E+07	3.67E–07	0.0023	1.58E–04	
	5–10 mm	2.45E+05	36	4.54E+06	144	87.4	1.42E+07	2.90E–07	0.0021	1.39E–04	
	10–15 mm	2.24E+05	36	4.15E+06	144	87.4	1.30E+07	2.65E–07	0.0020	1.35E–04	
	15–17.5 mm	1.33E+05	36	2.46E+06	144	87.4	7.71E+06	1.57E–07	0.0011	1.38E–04	
	17.5–20 mm	1.33E+05	36	2.47E+06	144	87.4	7.74E+06	1.58E–07	0.00109	1.45E–04	1.64E–04
T2 1750 (–) 123d											
	0–1 mm	2.65E+04	36	4.91E+05	144	87.4	1.54E+06	3.14E–08	0.0002	2.04E–04	
	1–5 mm	2.03E+05	36	3.75E+06	144	87.4	1.18E+07	2.40E–07	0.0021	1.16E–04	
	5–10 mm	1.63E+05	36	3.01E+06	144	87.4	9.43E+06	1.92E–07	0.0017	1.13E–04	
	10–15 mm	1.36E+05	36	2.52E+06	144	87.4	7.91E+06	1.61E–07	0.0015	1.05E–04	
	15–17.5 mm	1.28E+05	36	2.37E+06	144	87.4	7.43E+06	1.52E–07	0.0014	1.05E–04	
	17.5–20 mm	1.66E+05	36	3.07E+06	144	87.4	9.61E+06	1.96E–07	0.0018	1.09E–04	1.25E–04
T8 2000 (+) 47d											
	Sample 1, pos. 1	2.95E+04	36	5.47E+05	64	87.4	9.09E+05	1.85E–08	0.00021	8.84E–05	
	Sample 2, pos. 1	3.24E+04	36	6.00E+05	64	87.4	9.97E+05	2.03E–08	0.00021	9.70E–05	9.27E–05
	Sample 1, pos. 2	4.00E+04	36	7.41E+05	64	87.4	1.23E+06	2.51E–08	0.00021	1.21E–04	
	Sample 2, pos. 2	3.87E+04	36	7.16E+05	64	87.4	1.19E+06	2.43E–08	0.00022	1.11E–04	1.16E–04
	Sample 1, pos. 3	6.65E+04	36	1.23E+06	64	87.4	2.05E+06	4.18E–08	0.00021	2.01E–04	
	Sample 2, pos. 3	7.03E+04	36	1.30E+06	64	87.4	2.16E+06	4.41E–08	0.00022	2.02E–04	2.02E–04

Test cell code	Clay fraction	Counts per minute (cpm)	Instrument efficiency (%)	Disintegrations per second (dps)	Time elapsed since isotope preparation (days)	Half-life ^{35}S (days)	Normalized activity (dps) (Bq)	Amount ^{35}S (mmole)	Pore water volume (L)	Amount ^{35}S per liter (mM)	Average amount ^{35}S per liter (mM)
T9 2000 (+) 77d											
	0–1 mm	2.05E+04	36	3.80E+05	102	87.4	8.54E+05	1.74E–08	0.00010	1.75E–04	
	1–5 mm	1.44E+05	36	2.66E+06	102	87.4	5.97E+06	1.22E–07	0.00104	1.17E–04	
	5–10 mm	2.20E+05	36	4.08E+06	102	87.4	9.16E+06	1.87E–07	0.00147	1.27E–04	
	10–15 mm	2.29E+05	36	4.23E+06	102	87.4	9.51E+06	1.94E–07	0.00151	1.29E–04	
	15–17.5 mm	1.68E+05	36	3.10E+06	102	87.4	6.97E+06	1.42E–07	0.00065	2.17E–04	
	17.5–20 mm	2.89E+05	36	5.36E+06	102	87.4	1.20E+07	2.45E–07	0.00138	1.78E–04	1.57E–04
T10 2000 (+) 123d											
	0–1 mm	3.04E+04	36	5.63E+05	144	87.4	1.77E+06	3.60E–08	0.0003	1.34E–04	
	1–5 mm	1.18E+05	36	2.19E+06	144	87.4	6.87E+06	1.40E–07	0.0011	1.29E–04	
	5–10 mm	1.37E+05	36	2.53E+06	144	87.4	7.93E+06	1.62E–07	0.0012	1.31E–04	
	10–15 mm	1.28E+05	36	2.36E+06	144	87.4	7.40E+06	1.51E–07	0.0011	1.37E–04	
	15–17.5 mm	6.75E+04	36	1.25E+06	144	87.4	3.92E+06	7.99E–08	0.0006	1.28E–04	
	17.5–20 mm	3.28E+05	36	6.07E+06	144	87.4	1.90E+07	3.88E–07	0.0019	2.07E–04	1.44E–04
T6 2000 (−) 123d											
	0–1 mm	1.11E+04	36	2.05E+05	144	87.4	6.41E+05	1.31E–08	0.0001	1.47E–04	
	1–5 mm	1.28E+05	36	2.38E+06	144	87.4	7.45E+06	1.52E–07	0.0011	1.40E–04	
	5–10 mm	1.25E+05	36	2.31E+06	144	87.4	7.23E+06	1.48E–07	0.0010	1.43E–04	
	10–15 mm	1.34E+05	36	2.49E+06	144	87.4	7.79E+06	1.59E–07	0.0012	1.36E–04	
	15–17.5 mm	7.99E+04	36	1.48E+06	144	87.4	4.64E+06	9.46E–08	0.0007	1.31E–04	
	17.5–20 mm	1.10E+05	36	2.04E+06	144	87.4	6.38E+06	1.30E–07	0.0008	1.61E–04	1.43E–04
T7 2000 (−) 123d											
	0–1 mm	2.22E+04	36	4.11E+05	144	87.4	1.29E+06	2.63E–08	0.0002	1.35E–04	
	1–5 mm	1.56E+05	36	2.89E+06	144	87.4	9.05E+06	1.85E–07	0.0013	1.38E–04	
	5–10 mm	1.66E+05	36	3.08E+06	144	87.4	9.64E+06	1.97E–07	0.0016	1.24E–04	
	10–15 mm	1.88E+05	36	3.48E+06	144	87.4	1.09E+07	2.22E–07	0.0016	1.38E–04	
	15–17.5 mm	1.83E+05	36	3.39E+06	144	87.4	1.06E+07	2.17E–07	0.0013	1.64E–04	
	17.5–20 mm	1.63E+05	36	3.03E+06	144	87.4	9.48E+06	1.93E–07	0.0008	2.54E–04	1.59E–04

A.5 SO_4^{2-} in clay cores

Test cell code	Clay fraction	Analyzed SO_4^{2-} (mg/L)	Amount of SO_4^{2-} in test tube (mg/40 mL)	Amount of SO_4^{2-} in test tube (mole)	Amount of bentonite clay in test tube (gww)	Water content (%)	Pore water volume (L)	Amount of SO_4^{2-} per liter (mM)	Average amount of SO_4^{2-} per liter (mM)
T3 1750 (+) 47d									
	Sample 1, pos. 1	8	0.32	3.33E–06	1.21	31.93	0.00039	8.63	
	Sample 2, pos. 1	12	0.48	5.00E–06	1.07	31.93	0.00034	14.63	1.16E+01
	Sample 1, pos. 2	8	0.32	3.33E–06	1.01	31.93	0.00032	10.33	
	Sample 2, pos. 2	7	0.28	2.92E–06	1.00	31.93	0.00032	9.13	9.73E+00
	Sample 1, pos. 3	7	0.28	2.92E–06	1.01	31.93	0.00032	9.04	
	Sample 2, pos. 3	13	0.52	5.42E–06	1.06	31.93	0.00034	16.00	1.25E+00
T4 1750 (+) 77d									
	0–1 mm	1	0.04	4.17E–07	0.93	31.93	0.00030	1.40	
	1–5 mm	136	5.44	5.67E–05	5.48	31.93	0.00175	32.38	
	5–10 mm	114	4.56	4.75E–05	4.71	31.93	0.00150	31.58	
	10–15 mm	154	6.16	6.41E–05	6.11	31.93	0.00195	32.88	
	15–17.5 mm	88	3.52	3.67E–05	3.22	31.93	0.00103	35.65	
	17.5–20 mm	124	4.96	5.17E–05	4.39	31.93	0.00140	36.85	3.39E+01
T5 1750 (+) 123d									
	0–1 mm	18	0.72	7.50E–06	0.43	31.93	0.00014	54.61	
	1–5 mm	170	6.8	7.08E–05	6.15	31.93	0.00196	36.06	
	5–10 mm	130	5.2	5.42E–05	5.34	31.93	0.00171	31.76	
	10–15 mm	110	4.4	4.58E–05	5.23	31.93	0.00167	27.44	
	15–17.5 mm	110	4.4	4.58E–05	4.57	31.93	0.00146	31.40	
	17.5–20 mm	80	3.2	3.33E–05	3.28	31.93	0.00105	31.82	3.55E+01
T1 1750 (−) 123d									
	0–1 mm	12	0.48	5.00E–06	0.22	32.77	0.00007	69.34	
	1–5 mm	260	10.4	1.08E–04	7.10	32.77	0.00233	46.55	
	5–10 mm	220	8.8	9.16E–05	6.35	32.77	0.00208	44.04	
	10–15 mm	240	9.6	1.00E–04	5.99	32.77	0.00196	50.93	
	15–17.5 mm	130	5.2	5.42E–05	3.48	32.77	0.00114	47.49	
	17.5–20 mm	110	4.4	4.58E–05	3.33	32.77	0.00109	41.99	5.01E+01

Test cell code	Clay fraction	Analyzed SO_4^{2-} (mg/L)	Amount of SO_4^{2-} in test tube (mg/40 mL)	Amount of SO_4^{2-} in test tube (mole)	Amount of bentonite clay in test tube (gww)	Water content (%)	Pore water volume (L)	Amount of SO_4^{2-} per liter (mM)	Average amount of SO_4^{2-} per liter (mM)
T2 1750 (−) 123d									
	0–1 mm	23	0.92	9.58E–06	0.47	32.77	0.00015	62.20	
	1–5 mm	220	8.8	9.16E–05	6.33	32.77	0.00207	44.18	
	5–10 mm	160	6.4	6.66E–05	5.20	32.77	0.00170	39.11	
	10–15 mm	120	4.8	5.00E–05	4.71	32.77	0.00154	32.39	
	15–17.5 mm	110	4.4	4.58E–05	4.40	32.77	0.00144	31.78	
	17.5–20 mm	170	6.8	7.08E–05	5.48	32.77	0.00180	39.43	4.15E+01
T8 2000 (+) 47d									
	Sample 1, pos. 1	0	0	0.00E+00	1.01	20.76	0.00021	0.00	
	Sample 2, pos. 1	1	0.04	4.17E–07	1.01	20.76	0.00021	1.99	9.93E–01
	Sample 1, pos. 2	55	2.2	2.29E–05	1.00	20.76	0.00021	110.36	
	Sample 2, pos. 2	56	2.24	2.33E–05	1.05	20.76	0.00022	107.01	1.09E+02
	Sample 1, pos. 3	51	2.04	2.12E–05	1.00	20.76	0.00021	102.33	
	Sample 2, pos. 3	50	2	2.08E–05	1.05	20.76	0.00022	95.55	9.89E+01
T9 2000 (+) 77d									
	0–1 mm	2	0.08	8.33E–07	0.48	20.76	0.00010	8.36	
	1–5 mm	24	0.96	1.00E–05	5.01	20.76	0.00104	9.61	
	5–10 mm	400	16	1.67E–04	7.09	20.76	0.00147	113.20	
	10–15 mm	420	16.8	1.75E–04	7.26	20.76	0.00151	116.08	
	15–17.5 mm	180	7.2	7.50E–05	3.15	20.76	0.00065	114.66	
	17.5–20 mm	420	16.8	1.75E–04	6.64	20.76	0.00138	126.92	8.15E+01
T10 2000 (+) 123d									
	0–1 mm	9	0.36	3.75E–06	1.29	20.76	0.00027	14.00	
	1–5 mm	150	6	6.25E–05	5.22	20.76	0.00108	57.66	
	5–10 mm	270	10.8	1.12E–04	5.96	20.76	0.00124	90.90	
	10–15 mm	390	15.6	1.62E–04	5.30	20.76	0.00110	147.65	
	15–17.5 mm	110	4.4	4.58E–05	3.00	20.76	0.00062	73.57	
	17.5–20 mm	440	17.6	1.83E–04	9.05	20.76	0.00188	97.55	8.02E+01

Test cell code	Clay fraction	Analyzed SO_4^{2-} (mg/L)	Amount of SO_4^{2-} in test tube (mg/40 mL)	Amount of SO_4^{2-} in test tube (mole)	Amount of bentonite clay in test tube (gww)	Water content (%)	Pore water volume (L)	Amount of SO_4^{2-} per liter (mM)	Average amount of SO_4^{2-} per liter (mM)
T6 2000 (−) 123d									
	0–1 mm	3	0.12	1.25E–06	0.41	21.64	0.00009	14.08	
	1–5 mm	50	2	2.08E–05	5.03	21.64	0.00109	19.13	
	5–10 mm	230	9.2	9.58E–05	4.77	21.64	0.00103	92.82	
	10–15 mm	290	11.6	1.21E–04	5.40	21.64	0.00117	103.38	
	15–17.5 mm	150	6	6.25E–05	3.35	21.64	0.00072	86.19	
	17.5–20 mm	170	6.8	7.08E–05	3.73	21.64	0.00081	87.73	6.72E+01
T7 2000 (−) 123d									
	0–1 mm	7	0.28	2.92E–06	0.90	21.64	0.00019	14.97	
	1–5 mm	90	3.6	3.75E–05	6.19	21.64	0.00134	27.99	
	5–10 mm	330	13.2	1.37E–04	7.31	21.64	0.00158	86.90	
	10–15 mm	390	15.6	1.62E–04	7.46	21.64	0.00161	100.63	
	15–17.5 mm	300	12	1.25E–04	6.10	21.64	0.00132	94.67	
	17.5–20 mm	150	6	6.25E–05	3.52	21.64	0.00076	82.03	6.79E+01

Arkitektkopia AB, Bromma, 2015

SKB is tasked with managing Swedish nuclear and radioactive waste in a safe way.

skb.se